Hydrol. Earth Syst. Sci. Discuss., doi:10.5194/hess-2016-247, 2016
Manuscript under review for journal Hydrol. Earth Syst. Sci.
Published: 23 May 2016

Hydrology and Earth System Sciences
Open Access
EGU
Discussions

Comparison of six different soft computing methods in modeling evaporation in different climates

Lunche Wang[1], Ozgur Kisi[2], Mohammad Zounemat-Kermani[3], Yiqun Gan[4]

[1]Laboratory of Critical Zone Evolution, School of Earth Sciences, China University of Geosciences, Wuhan 430074, China;

[2]Canik Basari University, Faculty of Architecture and Engineering, Civil Engineering Department, Samsun, Turkey;

[3]Department of Water Engineering, Shahid Bahonar University of Kerman, Kerman, Iran;

[4]School of Enviromental studies, China University of Geosciences, Wuhan 430074, China;

Corresponding author: Lunche Wang, Laboratory of Critical Zone Evolution, School of Earth Sciences, China University of Geosciences, Lumo road 388, Hongshan District, Wuhan 430074, China; Tel.: +86 13349889828; E-mail address: wang@cug.edu.cn

Hydrol. Earth Syst. Sci. Discuss., doi:10.5194/hess-2016-247, 2016
Manuscript under review for journal Hydrol. Earth Syst. Sci.
Published: 23 May 2016

Hydrology and Earth System Sciences
Discussions

Abstract: Evaporation plays important roles in regional water resources management, terrestrial ecological process and regional climate change. This study investigated the abilities of six different soft computing methods, Multi-layer perceptron (MLP), generalized regression neural network (GRNN), fuzzy genetic (FG), least square support vector machine (LSSVM), multivariate adaptive regression spline (MARS), adaptive neuro-fuzzy inference systems with grid partition (ANFIS-GP), and two regression methods, multiple linear regression (MLR) and Stephens and Stewart model (SS) in predicting monthly *Ep*. Long-term climatic data at eight stations in different climates, air temperature (*Ta*), solar radiation (*Rg*), sunshine hours (*Hs*), relative humidity (*RH*) and wind speed (*Ws*) during 1961-2000 are used for model development and validation. The first part of applications focused on testing and comparing the model accuracies using different local input combinations. The results showed that the models have different accuracies in different climates and the MLP model performed superior to the other models in predicting monthly *Ep* at most stations, while GRNN model performed better in Tibetan Plateau. The accuracies of above models ranked as: MLP, GRNN, LSSVM, FG, ANFIS-GP, MARS and MLR. Generalized models were also developed and tested with data of eight stations. The overall results indicated that the soft computing techniques generally performed better than the regression methods, but MLR and SS models can be more preferred at some climatic zones instead of complex nonlinear models, for example, the BJ, CQ and HK stations.

Keywords: Pan evaporation; soft computing techniques; regression methods; model comparison

1. Introduction

Evaporation is the process of conversion of liquid water to water vapor, which depends on the differences in vapor pressure and air between the surface and surrounding atmosphere

Hydrol. Earth Syst. Sci. Discuss., doi:10.5194/hess-2016-247, 2016
Manuscript under review for journal Hydrol. Earth Syst. Sci.
Published: 23 May 2016

(Penman 1948; Kisi, 2013; Kim et al., 2015). Pan evaporation (*Ep*), which is a major component of hydrological cycle, plays important roles in scheduling water resources and designing of irrigation systems. It has been widely used as an index of lake and reservoir evaporation, potential or reference crop evapotranspiration and irrigation (Snyder 1993). There are many factors influencing the rates of *Ep*, including solar radiation (*Rg*), air temperature (*Ta*), relative humidity (*RH*), sunshine hours (*Hs*) and wind speed (*Ws*). The quantitative effects of different climatic parameters on *Ep* variations in different regions is still one of the less understood aspects in the hydrologic cycle. Therefore, proper estimation and prediction of *Ep* is of great importance to integrated water resources management and modeling studies.

The direct measurements of *Ep* are spatially and temporally limited due to some instrumental and practical issues (Shirsath and Singh, 2010; Shiri et al., 2014). Many researchers have tried to estimate the evaporation through indirect methods using climatic variables, for example, many empirical or semi-empirical equations have been developed for estimating *Ep* as a function of meteorological data (Stephens and Stewart 1963; Piri et al., 2009), but some of these techniques require the data which are often incomplete or not always available for many locations (Sharda et al., 2008; Majidi et al., 2015). Recently, the advanced soft computing techniques (such as artificial neural network, ANN) have been successfully applied for modeling *Ep* due to its ability to learn complex and non-linear relationships that are difficult to model with conventional techniques (Sudheer et al., 2002; Kisi and Ozturk, 2007; Kim and Kim, 2008; Kisi, 2009b; Rahimikhoob, 2009; Guven and Kisi, 2011; Kim et al., 2013; Goyal et al., 2014; Shiri et al., 2015; Kisi et al., 2016), for example, Kisi (2009a) investigated the abilities of three different ANN techniques and it was found that the MLP and radial basis neural network (RBNN) computing techniques could be employed successfully to model the evaporation process using the available climatic data; Piri et al. (2009) improved the ANN

Hydrol. Earth Syst. Sci. Discuss., doi:10.5194/hess-2016-247, 2016
Manuscript under review for journal Hydrol. Earth Syst. Sci.
Published: 23 May 2016

model by incorporating an autoregressive external input (ARX) component and evaluated the models for *Ep* estimation at a site in hot and dry climate of Southeast Iran. The results showed that NNARX is better than the ANN and Marciano method, the models with inputs of wind and vapor pressures performed much better than the ones with temperature and dew point; Chang et al. (2010) proposed a self-organizing map neural network (SOMN) to assess the variability of daily evaporation based on meteorological variables, the results demonstrated that the topological structures of SOMN could give a meaningful map to present the clusters of meteorological variables and the networks could well estimate the daily evaporation (Kim et al., 2015). Kim et al. (2012) applied multilayer perceptron-neural networks (MLP), generalized regression neural networks (GRNN) and support vector machine-neural networks (SVM) to estimate *Ep* in temperate and arid climatic zones and the results indicated that these ANN models performed better than the emprical Linacre model and MLR model. Goyal et al. (2014) investigated the abilities of ANN, Least Squares Support Vector Machine (LSSVM), Fuzzy Logic (FG), Adaptive Neuro-Fuzzy Inference System (ANFIS) techniques, Hargreaves and Samani method (HGS), as well as the Stephens-Stewart (SS) method to improve the accuracy of daily *Ep* estimation in sub-tropical climates of India. The results showed that the above soft computing models outperformed the HGS and SS methods, and the LSSVM and FG models produced the highest accuracies. Kisi (2015) investigated the accuracy of LSSVM, multivariate adaptive regression splines (MARS) and M5 Model Tree (M5Tree) in modeling *Ep* at Mersin and Antalya stations in Mediterranean region of Turkey, which indicated that the LSSVM model could be successfully used for estimating *Ep* using local input and output data while the MARS model performed better than the LSSVM model in case of without local input and outputs. Several studies have also been performed in order to compare and assess the *Ep* models with limited data around the world (Kisi and Cengiz, 2013; Majidi et al., 2015). On the contrary, only a few studies have been conducted to find the most appropriate methods

Hydrol. Earth Syst. Sci. Discuss., doi:10.5194/hess-2016-247, 2016
Manuscript under review for journal Hydrol. Earth Syst. Sci.
Published: 23 May 2016

to estimate *Ep*, and most of these studies focused on comparing only two or three models. Therefore, there is no clear consensus on which methods are better to employ when lacking important long term measured data such as radiation and heat fluxes. Meanwhile, the *Ep* models are only tested at few number of stations in literature, for example, Keskin et al. (2004) only compared the FG model with empirical Penman method at Lake Eğirdir in Turkey; Sanikhani et al. (2012) compared two different ANFIS models including grid partitioning (GP) and subtractive clustering (SC), in modeling *Ep* at San Francisco and San Diego in California, however, there are almost no studies using large number of stations (> 3) for obtaining more generalized conclusions. In addition, there are not any studies in literature that compare different methods in estimating *Ep* at different climates (for example, the arid continental climate, desert climate, semi humid monsoon climate, plateau climate and the tropical maritime monsoon climate), which provided an impetus for the present investigation for revealing a more robust and applicable *Ep* estimation model.

Considering the importance of the evaporation in either irrigation management or hydrological modeling, the aim of this study is to investigate capability and usability of six different soft computing methods, ANFIS-GP, FG, GRNN, LSSVM, MARS and MLP, and two regression methods, MLR and SS, in modeling *Ep* using different climatic input combinations of *Rg, Ta, Hs, RH* and *Ws*. Data from eight stations in different climatic zones are used for training and testing above models. The model performances will be compared and discussed through: (i) estimating *Ep* of each station using different local input combinations; (ii) estimating *Ep* of eight stations using generalized ANFIS-GP, FG, GRNN, LSSVM, MARS, MLP, MLR and SS models. To the knowledge of the authors, no similar studies have been reported using above mentioned methods for modeling *Ep*, this will be the first study to compare the accuracy of multiple soft computing models for *Ep* estimation in different climates.

Hydrol. Earth Syst. Sci. Discuss., doi:10.5194/hess-2016-247, 2016
Manuscript under review for journal Hydrol. Earth Syst. Sci.
Published: 23 May 2016

2. Methods and materials

2.1. Modeling strategies

2.1. 1. Multi-layer perceptron neural network

Fig. 1

MLP is well-known and efficient neural network widely used for a variety of problems such as classification, time series modeling and regression. MLPs are organized hierarchically networks by several layers, including an input layer, hidden layer(s) and an output layer (Zounemat-Kermani et al., 2013; Wang et al., 2016b). There are one or more hidden layers between the input and output layers which are connected by neurons (including synaptic weights, biases and activation or transfer functions). Each neuron receives its input value(s) from the input vector (or the antecedent hidden layer's output) and then calculates a weighted sum of input values passing through the transfer function, which generates the output of the neuron (Fig. 1a). MLPs are feed-forward networks, using the error back-propagation (BP) algorithm for network training. In the BP algorithm, an iterative process changes the weights and biases of the network to optimize the solution by reducing the overall error between the output and target (generally the observed parameters) values. More details about the MLP model can be found in Kisi (2009b) and Zounemat-Kermani (2012).

2.1. 2. Generalized regression neural network

The GRNN model has a parallel structure, but they do not use an iterative process for learning procedure between the input and output variables. The structure of GRNN consists of four consequent layers, namely the 1) input, 2) pattern, 3) summation, and 4) output layers (see Fig.1b for a schematic diagram of a GRNN network). In the first layer, the total number of input variables is equal to the number of input units. Input data are linked to the second layer where each neuron presents a training pattern. The second layer sends processed information

Hydrol. Earth Syst. Sci. Discuss., doi:10.5194/hess-2016-247, 2016
Manuscript under review for journal Hydrol. Earth Syst. Sci.
Published: 23 May 2016

to the third (summation) layer through the pattern neurons. In the summation layer, there are two types of S-summation and D-summation neurons, which are connected to the pattern layer unit (Zounemat-Kermani, 2014). The sum of the weighted responses of the second layer is calculated by the S-summation neurons, while the D-summation neurons compute the un-weighted outputs. Finally, in the output layer, the division of the output of each S-summation neuron by D-summation neuron gives the output value. More descriptions about the GRNN model can be seen from Cigizoglu and Alp (2006).

2.1. 3. Grid partitioning adaptive neuro-fuzzy inference system

Fig. 2

ANFIS refers to a multi-layer adaptive network combined with neural network analogy with the fuzzy inference system. It consists of five consecutive layers (fuzzification, product, normalization, de-fuzzification and output) in an implementation procedure of different node functions to learn and adjust the parameters in a fuzzy inference system (Fig. 2). A hybrid learning algorithm, including forward and backward passes is utilized for reducing calculated errors and training phase. With the calculation of the least squared error, the consequent parameters are updated, whereas, the premise parameters are fixed. Hence, in the backward pass the consequent parameters are fixed and the premise parameters are updated through the gradient descent algorithm (Kisi and Ozturk, 2007; Zounemat-Kermani and Teshnehlab, 2008; Khayam et al., 2012).

Membership functions and fuzzy inference parameters are identified according to the adjustment of premise and consequent parameters by an iterative process of the forward and backward passes. Construction of ANFIS models is based on the partitioning of the input-output data for establishing the rule base system. In this respect, various approaches such as ANFIS-GP, subtractive clustering and fuzzy c-means methods can be applied.

Hydrol. Earth Syst. Sci. Discuss., doi:10.5194/hess-2016-247, 2016
Manuscript under review for journal Hydrol. Earth Syst. Sci.
Published: 23 May 2016

In this study the Sugeno model, which is the most commonly used system, along with the grid partitioning method is applied for modelling evapotranspiration. The reader can find out more details about ANFIS-GP in several available publications (Jang, 1993; Terzi et al., 2006; Khayam et al., 2012).

2.1. 4. Fuzzy-genetic algorithm

The hybrid FG algorithm combines a meta-heuristic algorithm (genetic algorithm) and an adaptive fuzzy inference system (AFIS). In the AFIS, the input vectors along with the corresponding output(s) are introduced to the fuzzy system which is established based on the fuzzy logic approach. For further information about fuzzy logic, the reader is referred to related reports (Zounemat-Kermani and Scholz, 2013).

Genetic algorithms (GAs) are stochastic search algorithm based on the mechanics of natural genetics and natural selection which can be used for optimization problems. Getting the advantage of using the evolutionary mechanism, they are capable of searching large solution spaces efficiently. GA is composed of three main stages, namely, population initialization, GA operators (reproduction, crossover, and mutation) and evaluation (Kisi and Tombul, 2013). In this study, the proposed hybrid FG model is based on a model wherein the membership functions' parameters (e.g. center and width of Gaussian MFs) are optimized using a GA algorithm. The objective function of the genetic algorithm optimizer is the minimization of the error criterion (e.g. RMSE) of prediction made by an AFIS model (Kisi, 2009; Ganjidoost et al., 2015).

2.1. 5. Least-Squares support vector machine

The SVM is based on a statistical learning theory which projects the input data classes to a higher dimensional feature space. The aim of the SVM algorithm is searching for an optimum hyper-plane with the minimum distance to the observed values. The algorithm is efficient,

Hydrol. Earth Syst. Sci. Discuss., doi:10.5194/hess-2016-247, 2016
Manuscript under review for journal Hydrol. Earth Syst. Sci.
Published: 23 May 2016

quick and converging procedure to the global optimum (Mesbah et al., 2015; Lu et al., 2016). However, the SVM algorithm has been modified and improved, referring to the Least-Squares-SVM (LSSVM) (Suykens and Vandewalle, 1999). In addition to have all the merits of the original SVM, LSSVM has become simpler and more rapid. This issue is caused by the structure of the LSSVM algorithm which solves a group of linear equations instead of solving a quadratic programming problem in the SVM method. LSSVM gets the advantage of the applying equality constraints (in exchange for traditional inequality constraints of SVM) and implements the sum of squared regression errors in the training process. Further details about the main equations and complete explanations of this subject can be found in Suykens and Vandewalle (1999) and Kisi (2015).

2.1. 6. Multivariate adaptive regression splines

MARS, introduced by Friedman (1991), is categorized as a nonparametric regression method. MARS divides the space of each independent variable into split various regions called sub-regions. For each sub-region a unique mathematical regression equation is defined. A relationship is developed for each sub-region of the independent variable to the output (response) of the system based on the attained mathematical equation. This whole process is conducted by a stepwise procedure consists of backward and forward steps. In the forward step, a set of appropriate input variables is selected and split. However, split process in the forward step might generate an over-fitted complex model resulting in poor performance. Thereafter, in the backward step unnecessary variables will be eliminated (Adamowski et al., 2012; Kisi, 2015). For more detailed information on the development of the MARS models used throughout in this research the reader can refer to Shardaet al. (2008) and Kisi (2015).

2.1. 7. Multiple Linear Regressions

Hydrol. Earth Syst. Sci. Discuss., doi:10.5194/hess-2016-247, 2016
Manuscript under review for journal Hydrol. Earth Syst. Sci.
Published: 23 May 2016

MLR is a technique utilized to model the linear relationship between a dependent variable and one or more independent variables. The dependent variable is sometimes additionally called the predictors. MLR is depends on least squares: the model is fit such that the sum of squares of differences of estimated and observed values is minimized (http://tree.ltrr.arizona.edu/webhome/dmeko/geos585a.html#cLesson11). MLR is probably the most widely used method in hydrology and climatology for developing models to reconstruct or analysis the long-term variations of climatic factors in literature. In this study, MLR models are developed using the same data set which was used to train and test the above soft computing models.

2.1. 8. Stephens and Stewart Model

Stephens and Stewart (SS) model is an empirical linear equation and requires only radiation and temperature data (Stephens and Stewart 1963). This model was reported as the best among 23 models (Al-Shalan and Salih, 1987; Sudheer et al., 2002; Shirsath and Singh, 2010), which can be expressed as $Ep = Rg$ (a + $b \times Ta$), where a and b are fitting constants (determined on the training data through least square fitting).

2.2. Case study and data

Fig. 3

In this study, monthly climatic data at eight stations of China Meteorological Administration (CMA) were used for developing and testing *Ep* models in different climates. Fig.3 shows the detailed geographical locations of above stations, which are named as HEB (latitude 45°45′ N, longitude 126°46′E, 142.3 masl (m above sea level), ALT (47°44′ N, 188° 05′E, 735.3 masl), MQ (38°38′ N, 103°05′E, 1367 masl), BJ (39°48′ N, 116°28′E, 31.3 masl), LSA (29°40′ N, 91°08′E, 3648.7 masl), CQ (29°35′ N, 106°28′E, 259.1 masl), HZ (30°14′ N, 120°10′E, 41.7 masl) and HK (20°02′ N, 110°21′E, 13.9 masl). It should be noted that above stations are

Hydrol. Earth Syst. Sci. Discuss., doi:10.5194/hess-2016-247, 2016
Manuscript under review for journal Hydrol. Earth Syst. Sci.
Published: 23 May 2016

243 located at different climatic zones, for example, the HEB station is in the Northeast China
244 with long and cold winter (semi humid temperate continental climate); the ALT station is in
245 the Northwest China with arid continental climate; the MQ station is surrounded by the
246 Tengger and Badan Jilin desert, which is characterized by continental desert climate with hot
247 summer and cold winter, enough light and little rainfall amount; BJ is characterized by typical
248 north temperate semi humid continental monsoon climate; LSA is in the zone of semi-arid
249 plateau climate, which is called the sunlight city due to the sufficient sunshine resources in
250 Tibetan Plateau; CQ is characterized by subtropical monsoon humid climate with more
251 cloudy and foggy conditions; the HZ station is known as one of China's "four ovens" cities
252 where summertime temperatures can reach to 40 ^{o}C, which is characterized by hot and rainy
253 in summer, cold and dry in winter due to the effects of East Asian atmospheric circulation, the
254 terrain of Qinghai-Tibet Plateau and the North Pacific Ocean; the HK station is located at the
255 northern margin of the low latitude tropics, which belongs to the tropical maritime monsoon
256 climate. The detailed information about the geographical, climatic and hydrological
257 conditions in this region can also be seen in Zhai et al. (1999) and Ding et al. (2006).

258 Fig. 4

259 The data used in this research cover 40 years (1961-2000) of monthly records of air
260 temperature (*Ta*), solar radiation (*Rg*), sunshine durations (*Hs*), relative humidity (*RH*), wind
261 speed (*Ws*) and pan evaporation (*Ep*). For each station, 50% of the whole data were randomly
262 chosen for training the *Ep* models and the remaining data were used for testing the models.
263 The annual variations of *Ep* and associated climatic factors are shown clearly in Fig. 4, it is
264 clear that *Ep* at MQ and LSA are generally higher than those at other stations, there are
265 decreasing trends of *Ep* for ALT, BJ and HK stations during 1960-2000, and the most
266 significant increasing trends of *Ep* are observed for LSA station. The *Hs* at CQ and HZ
267 stations are much lower than those at other stations and the annual mean *Hs* is the highest

Hydrol. Earth Syst. Sci. Discuss., doi:10.5194/hess-2016-247, 2016
Manuscript under review for journal Hydrol. Earth Syst. Sci.
Published: 23 May 2016

among the eight stations. There are also slight increasing trends for *Hs* at most stations except BJ, HK and HZ stations. The annual mean *Rg* is obviously higher at LSA station and *Rg* at CQ is the lowest, the *Rg* generally decreased from 1961 to 1990 and then increased for most stations. The *RH* is generally larger than 75% at HZ, CQ and HK stations and lower than 50% for MQ and LSA stations. There are distinct differences for annual mean *Ta* at above eight stations, for example, *Ta* at HK is generally higher than 23 ^{o}C, while the highest annual mean *Ta* at HEB is lower than 5 ^{o}C. However, *Ws* is highest at HEB and lowest at CQ station, and *Ws* is decreasing from 1960s to 2000s at most stations.

Table 1

Fig. 5

Table 1 showed the monthly statistics of the climatic parameters, x_{mean}, S_x, C_v, C_x, x_{min} and x_{max} denote the mean, standard deviation, variation coefficient, skewness, minimum and maximum values, respectively. It is clear that the monthly mean *Ep* is 4.35, 4.72, 7.26, 5.09, 6.35, 2.86, 3.65 and 5.00 mm for station HEB, ALT, MQ, BJ, LSA, CQ, HZ and HK, respectively. The mean *Rg* at LSA, MQ and ALT (20.41, 16.41 and 15.13MJ m^{-2}) are higher than those at other stations; the mean *Ta* at HK station is 24.08^{o}C, which is highest among all the stations. The *Hs* shows low variations for the MQ, BJ and LSA stations (see Cv values in Table1) and the monthly mean *Hs* at CQ (2.83 hour) is much lower than the other station. The monthly *RH* is 65.44%, 57.99%, 44.82%, 57.29%, 44.39%, 79.15%, 78.04% and 84.14% for HEB, ALT, MQ, BJ, LSA, CQ, HZ and HK, respectively, which indicates that *RH* is generally higher at lower latitudes. The *Ws* at HEB station is higher than other station in each month and the lowest monthly *Ws* (1.36 m s^{-1}) is observed at CQ station. The monthly *Ep*, *Ta*, *Hs* and *Rg* are generally higher in summer and lower in winter months (Fig.5); the *RH* is also lower in spring months for some stations such as HEB and MQ; the *Ws* is higher at spring and lower in summer months for most stations (Fig.5). For the HEB station, *RG* shows low

Hydrol. Earth Syst. Sci. Discuss., doi:10.5194/hess-2016-247, 2016
Manuscript under review for journal Hydrol. Earth Syst. Sci.
Published: 23 May 2016

skewed distribution and has a relatively higher correlation with *Ep* (R =0.89); the *RH* and *Ws* data have the lowest (R = -0.30, 0.26) correlation with *Ep*. For the ALT station, the *Ta* data have a high skewness (C_v =3.07) and high correlation with *Ep* (R =0.93). For the MQ station, the *Hs* shows the lower skewed distribution (C_v =0.13) and has a positive correlation with *Ep* (R = 0.72); the *Ta* data have a higher skewness (C_v =1.36) and the highest correlation with *Ep* (R =0.93). In similar, the *Rg* and *Hs* data show relatively higher skewness and correlations with *Ep* for the BJ, CQ and HK stations. At some cases, the correlations between *Ta* and *Ep* are also higher than those with *Hs*, for example, the LSA (R =0.75) and HZ (R =0.88) stations. It is clear from the statistical indices in Table 1 that each climatic variable have different correlations with *Ep*, and *Rg*, *Hs* and *Ta* variables seem to be the most effective parameters for predicting *Ep* with respect to the correlations.

2.3. Evaluation criteria

In this study, the ANFIS-GP, FG, GRNN, LSSVM, MARS, MLP, MLR and SS models were evaluated and compared with each other utilizing the mean absolute errors (MAE), root mean square errors (RMSE) and determination coefficient (R^2), which can be expressed as

$$RMSE = \sqrt{\frac{1}{N}\sum_{i=1}^{N}\left(Ep_{m,i} - Ep_{o,i}\right)^2} \quad (1)$$

$$MAE = \frac{1}{N}\sum_{i=1}^{n}\left|Ep_{m,i} - Ep_{o,i}\right| \quad (2)$$

$$R^2 = \frac{(\sum_{i=1}^{n}\left(Ep_{m,i} - \overline{Ep_m}\right)\left(Ep_{o,i} - \overline{Ep_o}\right))^2}{\sum_{i=1}^{n}\left(Ep_{m,i} - \overline{Ep_m}\right)^2 \sum_{i=1}^{n}\left(Ep_{o,i} - \overline{Ep_o}\right)^2} \quad (3)$$

where N and bar respectively indicate the number of data and mean of the variable, Ep_m and Ep_o are the modeled and observed pan evaporation.

Hydrol. Earth Syst. Sci. Discuss., doi:10.5194/hess-2016-247, 2016
Manuscript under review for journal Hydrol. Earth Syst. Sci.
Published: 23 May 2016

3. Results and discussion

This study compares six different soft computing methods, ANFIS-GP, FG, GRNN, LSSVM, MARS and MLP, and two empirical methods, MLR and SS, in modeling *Ep* using climatic inputs of *Rg, Ta, Hs, RH* and *Ws*. Data from eight stations, HEB, ALT, MQ, BJ, LSA, CQ, HZ and HK were utilized in the applications. The input combinations used for each model are provided in Table 2, the numbers after each model indicates the input combination. Two Gaussian membership functions were utilized for each ANFIS-GP and FG model. Different regularization constants and RBF kernel widths were tried for the LSSVM models and the optimal models that provided the least RMSE error in testing stage were obtained. For the GRNN models, different spread constants were tried. Different hidden node numbers were tried and the optimal ones were obtained for each MLP model.

Table 2

Table 3

Table 4

The training and testing results of the ANFIS-GP, FG, GRNN, LSSVM, MARS, MLP, SS and MLR models in predicting *Ep* of HEB station are shown in Table 3. It is clear from the table that the models with full weather data (*Rg, Ta, Hs, RH* and *Ws*) have the best accuracy. The MLP7 model performs superior to the other models in predicting *Ep* at HEB. The accuracy ranks of the applied soft computing models in testing period are: MLP, ANFIS-GP, FG, GRNN, MARS, LSSVM and MLR. It is clear from the first three input combinations that there is a slight difference between *Rg* and *Ta* and they are much more effective on modeling *Ep* at HEB station than the other variables. This is also confirmed by the R^2 values given in Table 1. Comparisons of the simple two-input (*Rg* and *Ta*) models clearly indicate that the ANFIS-GP4, GRNN4 and LSSVM4 models have better accuracy than those of the SS model while the FG4, MARS4 and MLP4 models give inferior results in testing period. Table 4

Hydrol. Earth Syst. Sci. Discuss., doi:10.5194/hess-2016-247, 2016
Manuscript under review for journal Hydrol. Earth Syst. Sci.
Published: 23 May 2016

gives the accuracy of the applied models in predicting *Ep* at ALT station. Similar to the HEB station, the models comprising whole weather inputs generally provide the best accuracy and the optimal MLP7 model outperforms the other models in predicting *Ep* at ALT station. The accuracy ranks of the models in testing stage are: MLP, LSSVM, ANFIS-GP, FG, MARS, GRNN and MLR. There is a slight difference between the *Rg*, *Ta* and *Hs* parameters and these are also parallel to the correlations given in Table 1. Two-input soft computing models seem to have a better accuracy than the SS model in predicting *Ep* at ALT station in the testing stage.

Table 5

Table 6

The training and testing statistics of the soft computing models, SS and MLR in predicting *Ep* of MQ station are provided in Table 5. In this station, five-input models also have the best performance and the MLP7 model performs superior to the other models. The accuracy ranks of the 5-input models are: MLP, FG, ANFIS-GP, GRNN, MARS, MLR and LSSVM. From the first three inputs, it is clear that the *Rg* and *Ta* variables have more effects on *Ep* than the *Hs* in MQ station. The correlations in Table 1 also confirm these results. It is apparent from Table 5 that the SS model provides inferior results in comparison with the 2-input soft computing models at MQ station. Table 6 reports the training and testing results of the applied models in predicting *Ep* at BJ station. From the table, it is obvious that the models with full weather data generally have the best accuracy. The MLP model provides better performance than the other models with respect to MAE, RMSE and R^2. The ranks of the applied models in testing accuracy are: MLP, LSSVM, GRNN, ANFIS-GP, FG, MARS and MLR. It is clear from the first three input combinations that the *Rg* which has a higher correlation with *Ep* (see Table 1) is much more effective on *Ep* than the *Ta* and *Hs* at BJ. Simple SS model seems to

Hydrol. Earth Syst. Sci. Discuss., doi:10.5194/hess-2016-247, 2016
Manuscript under review for journal Hydrol. Earth Syst. Sci.
Published: 23 May 2016

have better accuracy than the applied 2-input soft computing models in predicting *Ep* at BJ station in testing stage.

Table 7

Table 8

Table 7 compares the accuracy of the applied soft computing models in predicting *Ep* at LSA station. Similar to the previous stations, the best accuracies were generally obtained from five-input models and the GRNN model performs better than the other models with respect to MAE and RMSE statistics. The accuracies of the applied models in testing stage rank as: GRNN, MLP, LSSVM, MARS, FG, ANFIS-GP and MLR. The *Ta* seems to be the most effective parameter in predicting *Ep* at this station, which is also confirmed by the high correlation between *Ta* and *Ep* given in Table 1. The models with *Hs* input generally provide worse results than those comprising *Rg* input parameter. Two-input LSSVM4, ANFIS-GP4 and SS models have similar accuracy and they perform inferior to the FG4, GRNN4, MARS4 and MLP4 models. The accuracies of the ANFIS-GP, FG, GRNN, LSSVM, MARS, MLP, SS and MLR models in both training and testing stages are given in Table 8 for predicting *Ep* of CQ station. Unlike the previous stations, four-input models generally provide the best performance in this station. This implies that adding *Ws* input generally decreases the model accuracies even though it does not have a low correlation (R=0.58) with *Ep* at CQ station. The MLP6 and GRNN6 models have similar accuracies and they perform superior to the other models. The accuracy ranks of the above applied models in testing stage are: MLP, GRNN, FG, LSSVM, MARS, ANFIS-GP and MLR. Similar to the BJ station, the *Rg* input seems to have more effects on *Ep* than the *Ta* and *Hs* input at CQ station than the other variables even though the *Hs* has a higher correlation with *Ep*. Comparison of two-input models obviously shows that the SS model has a better accuracy than those of the other two-input soft computing models in testing period.

Hydrol. Earth Syst. Sci. Discuss., doi:10.5194/hess-2016-247, 2016
Manuscript under review for journal Hydrol. Earth Syst. Sci.
Published: 23 May 2016

387 Table 9

388 Table 10

389 The training and testing accuracy of the soft computing models, SS and MLR in predicting *Ep*
390 of HZ station are provided in Table 9. In this station, four- and five-input models also have
391 the best accuracies. The optimal MLP and GRNN models have similar performance and they
392 perform superior to the other models in predicting *Ep* at HZ station. The performance ranks of
393 the optimal models are: MLP, GRNN, MARS, FG, LSSVM, ANFIS-GP and MLR. Similar to
394 the BJ station, the *Rg* variable which has a higher correlation with *Ep* (see Table 1) is much
395 more effective on estimating *Ep* than the *Ta* and *Hs* at HZ. *Ta* variable also provides better
396 accuracy than the *Hs* in predicting *Ep*. Comparisons of simple two-input models clearly
397 indicates that the MARS4 and MLP4 models have better accuracy than those of the SS model
398 while the ANFIS-GP4, FG4, GRNN4 and LSSVM4 provide inferior results in testing stage.
399 Table 10 compares the accuracy of the models in predicting *Ep* at HK station. From the table,
400 it is clear that the best accuracies were obtained from five-input models in predicting *Ep*. The
401 MLP model performs superior to the other models with respect to MAE, RMSE and R^2
402 statistics. The accuracies of the applied models in testing period rank as: MLP, MLR, GRNN,
403 MARS, LSSVM, ANFIS-GP and FG. The accuracies of the MLR and MLP model are close
404 to each other. Therefore, simple MLR model can be preferred instead of more complex soft
405 computing models in predicting *Ep* at HK station. Unlike the previous stations, the models
406 comprising *Hs* input provide better accuracy than those which use only *Rg* or *Ta* input. The
407 *Rg* variable also seems to be more effective on *Ep* than the *Ta* at HZ station. The difference
408 among the two-input models is very small and the GRNN4 and SS models perform slightly
409 better than the other two-input models in predicting *Ep* at HK station.
410 It can be seen from above analysis that adding *RH* or *Ws* inputs into the applied models
411 generally increased their accuracies in predicting *Ep* in all stations even though these

Hydrol. Earth Syst. Sci. Discuss., doi:10.5194/hess-2016-247, 2016
Manuscript under review for journal Hydrol. Earth Syst. Sci.
Published: 23 May 2016

Hydrology and Earth System Sciences
Discussions

parameters had the lowest correlation with *Ep* (see Table 1). This indicates the non-linear relationship between *RH* (*Ws*) and *Ep* and linear R^2 indicator cannot show this phenomenon. General accuracies of the applied models are compared in Table 11. It is obvious that the MLP model provides much better scores than the other methods in predicting *Ep* at above eight stations (and data from all station) and the final accuracy ranks of the above models are: MLP, GRNN, LSSVM, FG, ANFIS-GP, MARS and MLR. In some stations (e.g., BJ, CQ), simple SS model performed superior to the two-input soft computing models and it can be preferred in these stations where *Hs, RH* and *Ws* parameters are not available.

Table 11

Figs.6-13 illustrates the estimates of the optimal models in testing phase for eight stations in the form of scatterplot. For HEP station, the fit line of the MARS model seems to be closer to the ideal line (y=x) while the MLP model has the highest R^2 means less scattered estimates than the other models. All the soft computing models provide close estimates to the corresponding observed ones in ALT station while MLR generally tends to overestimation. For MQ station, the LSSVM, MARS and MLR models provide more scattered estimates than the ANN (MLP and GRNN) and fuzzy based ANFIS-GP and FG models. All the models generally have good estimates at the BJ, CQ, HK and HZ stations. In LSA station, the MLP, GRNN, LSSVM and MARS provide less scattered estimates than the fuzzy based ANFIS-GP, FG and MLR models. From Figs.6-13, it is clear that the MLP model generally provided less scattered estimates than the other models in all stations. The models generally provided the worst accuracy in LSA station. One of the main reasons of this may be the fact that the *Ep* has low correlations with the climatic input data at LSA in comparison with other stations. It is clear from Fig. 12 that the SS model provides less scattered estimates for the ALT, CQ and HZ in comparison with other stations.

Fig. 6

Hydrol. Earth Syst. Sci. Discuss., doi:10.5194/hess-2016-247, 2016
Manuscript under review for journal Hydrol. Earth Syst. Sci.
Published: 23 May 2016

Fig. 7

Fig. 8

Fig. 9

Fig. 10

Fig. 11

Fig. 12

Fig. 13

The *Ep* data at all stations are further estimated using single generalized MLP, GRNN, MARS, LSSVM, ANFIS-GP, FG, MLR and SS models. The optimal models are obtained using training and testing data of above eight stations, the training and testing statistics of the applied models are compared in Table 12. Similar to the previous results, the best accuracies are obtained from the five-input models and the MLP model performs better than the other models. The accuracies of the applied models in testing stage rank as: MLP, GRNN, LSSVM, FG, ANFIS-GP, MARS and MLR. The *Rg* variable seems to be the most effective parameter in predicting *Ep* for data from all station, and the models with *Hs* input generally provides slightly better results than those comprising *Ta* input parameter. Two-input MARS4 and ANFIS-GP4 models perform inferior to the FG4, GRNN4, LSSVM4 and MLP4 models; the SS model has a lower accuracy than those of the other two-input soft computing models in testing period (Table 12). It is also observed that only *Ta* or *Hs* input seems to be insufficient for obtaining an accurate generalized *Ep* model and the model performances generally increase with input numbers, which implies that all above climatic parameters have positive effects on estimating *Ep* for most stations in different climates. The estimates of the generalized models are illustrated in Figs.6-13 (see the last scatterplot in each figure). It is clearly observed from the figures that the generalization significantly decreases models accuracy in estimating *Ep* at all stations. However, all the soft computing models generally

Hydrol. Earth Syst. Sci. Discuss., doi:10.5194/hess-2016-247, 2016
Manuscript under review for journal Hydrol. Earth Syst. Sci.
Published: 23 May 2016

462 have good generalization ability. Some underestimations of the high Ep values are clearly
463 seen for the generalized models. Different data ranges in training and test stages may be the
464 reason of this.

465 Table 12

466

467 **4. Conclusion**

468 This study investigated and compared the abilities of six different soft computing techniques,
469 MLP, GRNN, LSSVM, FG, ANFIS-GP, MARS, and two regression methods, MLR and SS,
470 in modeling *Ep* using different climatic input combinations of *Rg, Ta, Hs, RH* and *Ws*. The
471 climatic data obtained from eight stations in different climatic zones were used as inputs for
472 training and testing above models. In the first part of applications, the models with different
473 local input combinations were compared with each other in estimating *Ep* at each station,
474 separately. The results showed that the models with more inputs generally have better
475 accuracies and the MLP model performed superior to the other models in predicting monthly
476 *Ep* at most stations, however, the GRNN model performed better than the other models at
477 LSA station with respect to MAE and RMSE statistics. The *Rg* and *Ta* variables are more
478 effective on modeling *Ep* at most stations, while *Ta* seems to be the most important parameter
479 in predicting *Ep* at LSA, and adding *Ws* to the input combinations even decreases the model
480 accuracies. Sometimes, MLR model can be used for predicting *Ep* in tropic climate instead of
481 more complex soft computing models, and SS model can also be adopted for some stations in
482 regions of subtropical humid climate or temperate continental climate. The second part of
483 applications focused on estimating *Ep* of all stations using generalized models, which could
484 be successfully used for predicting *Ep* using different input combinations. The accuracies of
485 the applied models rank as: MLP, GRNN, LSSVM, FG, ANFIS-GP, MARS and MLR. The

Rg and *Hs* variables seem to be the most effective parameters in predicting *Ep* for data from all stations.

In summary, it is revealed in this study that the MLP models are the most appropriate for predicting *Ep* using limited climatic inputs in different climates. The present applications can be practically adopted in the field of water resources management for accurately mapping regional and global distributions of evaporation and related water resource storages.

Acknowledgement

This work was financially supported by the Special Fund for Basic Scientific Research of Central Colleges, China University of Geosciences, Wuhan (No.CUG150631), and the 111 Project (grant No. B08030). We would like to thank the China Meteorological Administration (CMA) for providing the meteorological and radiation data.

References

Adamowski, J., Chan, H.F., Prasher, S.O., Sharda, V.N., 2012. Comparison of multivariate adaptive regression splines with coupled wavelet transform artificial neural networks for runoff forecasting in Himalayan micro-watersheds with limited data. J. Hydroinfor. 14(3), 731-744.

Chang, F.G., Chang, L.C., Kao, H.S., Wu, G.R., 2010. Assessing the effort of meteorological variables for evaporation estimation by self-organizing map neural network, J. Hydrol. 384, 118-129.

Cigizoglu, H.K., Alp, M., 2006. Generalized regression neural network in modelling river sediment yield. Adv. Eng. Soft. 37(2), 63-68.

Ding, Y.H., Ren, G. Y., Shi, G.Y., Gong, P., Zheng, X.H., Zhai, P.M., Luo, Y., 2006. National assessment report of climate change (I): climate change in China and its future trend. Adv. Clim. Change Res. 2(1), 3-8.

510 Friedman, J. H., 1991. Multivariate adaptive regression splines. The annals of statistics, 1-67.

511 Ganjidoost, H., Mousavi, S.J., Soroush, A., 2015. Adaptive Network-Based Fuzzy Inference
512 Systems Coupled with Genetic Algorithms for Predicting Soil Permeability Coefficient.
513 Neural Proce. Lett. 1-27.

514 Goyal, M.K., Bharti, B., Quilty, J., Adamowski, J., Pandey, A., 2014. Modeling of daily pan
515 evaporation in sub-tropical climates using ANN, LS-SVR, Fuzzy Logic, and ANFIS. Expert
516 Syst. Appl. 41 (11), 5267-5276.

517 Guven, A., Kisi, O., 2011. Daily pan evaporation modeling using linear genetic programming
518 technique. Irrig. sci. 29(2),135-145.

519 Jang, J.S.R., 1993. ANFIS: adaptive-network-based fuzzy inference system. IEEE Trans.
520 Syst. Man Cybern. B 23(3), 665-685.

521 Keskin, M.E., Terzi, O., Taylan, D., 2004. Fuzzy logic model approaches to daily pan
522 evaporation estimation in western Turkey. Hydrol. Sci. J. 49 (6), 1001–1010.

523 Khayyam, H., Nahavandi, S., Davis, S., 2012. Adaptive cruise control look-ahead system for
524 energy management of vehicles. Expert sys. appl. 39(3), 3874-3885.

525 Kim, S., Kim, H.S., 2008. Neural networks and genetic algorithm approach for nonlinear
526 evaporation and evapotranspiration modeling. J. Hydrol. 35, 299-317.

527 Kim, S., Shiri, J., Kisi, O., 2012. Pan evaporation modeling using neural computing approach
528 for different climatic zones. Water Resour. Manage. 26(11), 3231-3249.

529 Kim, S., Shiri, J., Kisi, Ö., Singh, V. P. 2013. Estimating daily pan evaporation using different
530 data-driven methods and lag-time patterns. Water Resour. Manage. 27(7), 2267-2286.

531 Kim, S., Shiri, J., Singh, V. P., Kisi, Ö., Landeras, G., 2015. Predicting daily pan evaporation
532 by soft computing models with limited climatic data. Hydrol. Sci. J. 60(6), 1120-1136.

533 Kisi, O., Ozturk, O., 2007. Adaptive neurofuzzy computing technique for evapotranspiration
534 estimation. J. irrig. drainage eng. 133 (4), 368-379.

Kisi, O., 2009a. Daily pan evaporation modelling using multi-layer perceptrons and radial basis neural networks. Hydrol. process. 23 (2), 213-223.

Kisi, O., 2009b. Fuzzy genetic approach for modeling reference evapotranspiration. J. irrig. drainage eng. 136(3), 175-183.

Kisi, O., Cengiz, T.M., 2013. Fuzzy genetic approach for estimating reference evapotranspiration of Turkey: Mediterranean Region. Water Resour. Manag. 27, 3541-3553.

Kisi, O., Tombul, M., 2013. Modeling monthly pan evaporations using fuzzy genetic approach. J. Hydrol. 477, 203-212.

Kisi, O., 2015. Pan evaporation modeling using least square support vector machine, multivariate adaptive regression splines and M5 model tree. J. Hydrol. 528, 312-320.

Kisi, O., Genc, O., Dinc, S., Zounemat-Kermani, M., 2016. Daily pan evaporation modeling using chi-squared automatic interaction detector, neural networks, classification and regression tree. Comput. Elect. Agr. 122, 112-117.

Li, Z., Chen, Y., Shen, Y., Liu, Y., Zhang, S., 2013. Analysis of changing pan evaporation in the arid region of Northwest China. Water Res. Res. 49(4), 2205-2212.

Lin, G.F., Lin, H.Y., Wu, M.C., 2013. Development of a support-vector-machine-based model for daily pan evaporation estimation. Hydrol. Process. 27 (22), 3115-3127.

Lu, C., Chen, J., Hong, R., Feng, Y., Li, Y., 2016. Degradation trend estimation of slewing bearing based on LSSVM model. Mech. Sys. Sig. Process. 76, 353-366.

Majidi, M., Alizadeh, A., Farid, A., Vazifedoust, M., 2015. Estimating Evaporation from Lakes and Reservoirs under Limited Data Condition in a Semi-Arid Region. Water Resour. Manage. 29(10), 3711-3733.

Mesbah, M., Soroush, E., Azari, V., Lee, M., Bahadori, A., Habibnia, S., 2015. Vapor liquid equilibrium prediction of carbon dioxide and hydrocarbon systems using LSSVM algorithm. J. Supercri. Fluids, 97, 256-267.

Hydrol. Earth Syst. Sci. Discuss., doi:10.5194/hess-2016-247, 2016
Manuscript under review for journal Hydrol. Earth Syst. Sci.
Published: 23 May 2016

560 Piri, J., Amin, S., Moghaddamnia, A., Keshavarz, A., Han, D., Remesan, R., 2009. Daily pan
561 evaporation modeling in a hot and dry climate. J. Hydrol. Engin. 14(8), 803-811.
562 Rahimikhoob, A., 2009. Estimating daily pan evaporation using artificial neural network in a
563 semi-arid environment. Theoret. Appl. Climatol. 98(1-2), 101-105.
564 Sanikhani, H., Kisi, Ö., Nikpour, M.R., Dinpashoh, Y., 2012. Estimation of daily pan
565 evaporation using two different adaptive neuro-fuzzy computing techniques. Water Resour.
566 Manage. 26(15), 4347-4365.
567 Sharda, V.N., Prasher, S.O., Patel, R.M., Ojasvi, P.R., Prakash, C., 2008. Performance of
568 Multivariate Adaptive Regression Splines (MARS) in predicting runoff in mid-Himalayan
569 micro-watersheds with limited data. Hydrol. Sci. J. 53(6), 1165-1175.
570 Shiri, J., Sadraddini, A.A., Nazemi, A.H., Kisi, O., Landeras, G., Fakheri Fard, A., Marti, P.,
571 2014. Generalizability of gene expression programming-based approaches for estimating
572 daily reference evapotranspiration in coastal stations of Iran. J. Hydrol. 508, 1-11.
573 Shiri, J., Marti, P., Nazemi, A.H., Sadraddini, A.A., Kisi, O., Landeras, G., Fakheri Fard, A.,
574 2015. Local vs. external training of neuro-fuzzy and neural networks models for estimating
575 reference evapotranspiration assessed through k-fold testing. Hydrol. Res. 46(1), 72-88.
576 Shirsath, P. B., Singh, A. K., 2010. A comparative study of daily pan evaporation estimation
577 using ANN, regression and climate based models. Water Resour. Manage. 24(8), 1571-1581.
578 Stephens, J.C., Stewart, E.H., 1963 A comparison of procedures for computing evaporation
579 and evapotranspiration. Publication 62, international association of scientific hydrology.
580 International Union of Geodynamics and Geophysics, Berkeley, CA, pp. 123-133.
581 Suykens, J. A., Vandewalle, J., 1999. Least squares support vector machine classifiers. Neural
582 Process. Lett. 9(3), 293-300.
583 Sudheer, K.P., Gosain, A.K., Rangan, D.M., Saheb, S.M., 2002. Modelling evaporation using
584 an artificial neural network algorithm. Hydrol. Process. 16, 3189–3202.

585 Terzi, O., ErolKeskin, M., Dilek Taylan, E., 2006. Estimating evaporation using ANFIS. J.
586 irrig. drainage eng. 132(5), 503-507.
587 Terzi, O., Keskin, M.E., 2010. Comparison of artificial neural networks and empirical
588 equations to estimate daily pan evaporation. Irrig. Drain. 59, 215-225.
589 Wang, L., Kisi, O., Zounemat-Kermani, M., Hu, B., Gong, W., 2016. Modeling and
590 comparison of hourly photosynthetically active radiation in different ecosystems. Renew.
591 Sust. Energ. Reviews 56, 436-453.
592 Wang, L., Kisi, O., Zounemat-Kermani, M., Salazar, G. A., Zhu, Z., Gong, W., 2016. Solar
593 radiation prediction using different techniques: model evaluation and comparison. Renew.
594 Sust. Energ. Reviews 61, 384-397.
595 Zounemat-Kermani, M., 2012. Hydrometeorological parameters in prediction of soil
596 temperature by means of artificial neural network: Case study in Wyoming. J. Hydrol. Eng.
597 18(6), 707-718.
598 Zounemat-Kermani, M., 2014. Principal component analysis (PCA) for estimating
599 chlorophyll concentration using forward and generalized regression neural networks. Appl.
600 Artif. Intel. 28 (1), 16-29.
601 Zounemat-Kermani, M., Scholz, M., 2013. Modeling of dissolved oxygen applying stepwise
602 regression and a template-based fuzzy logic system. J. Environ. Eng. 140(1), 69-76.
603 Zounemat-Kermani, M., Teshnehlab, M., 2008. Using adaptive neuro-fuzzy inference system
604 for hydrological time series prediction. Appl. Soft Comput. 8(2), 928-936.
605 Zounemat-Kermani, M., Kisi, O., Rajaee, T., 2013. Performance of radial basis and LM-feed
606 forward artificial neural networks for predicting daily watershed runoff. Appl. Soft Comput.
607 13(12), 4633-4644.
608 Zhai, P., Sun, A., Ren, F., Liu, X., Gao, B., Zhang, Q. 1999. Changes of climate extremes in
609 China. In Weather and Climate Extremes (pp. 203-218). Springer Netherlands.

Hydrol. Earth Syst. Sci. Discuss., doi:10.5194/hess-2016-247, 2016
Manuscript under review for journal Hydrol. Earth Syst. Sci.
Published: 23 May 2016

Hydrology and Earth System Sciences
Discussions
Open Access
EGU

610 Table 1.Monthly statistical parameters of each data set for each station

Station	Dataset	x_{mean}	S_x	C_v	C_x	x_{min}	x_{max}	R		
HEB	***Rg***	12.98	5.35	0.41	0.00	3.68	28.71	0.89		
	Ta	4.17	14.52	3.48	-0.25	-24.71	25.25	0.86		
	Hs	7.02	1.59	0.23	-0.25	2.82	10.89	0.79		
	RH	65.44	11.01	0.17	-0.44	36.23	85.06	-0.36		
	Ws	3.69	0.97	0.26	0.61	1.88	6.69	0.26		
	E_P	4.35	3.27	0.75	0.44	0.16	12.96	1		
ALT	***Rg***	15.13	7.21	0.48	-0.06	2.34	27.69	0.92		
	Ta	4.54	13.95	3.07	-0.25	-25.08	24.87	0.93		
	Hs	8.2	2.52	0.31	-0.25	1.92	12.66	0.90		
	RH	57.99	13.41	0.23	0	30.1	86.77	-0.89		
	Ws	2.40	0.99	0.41	0.05	0.31	5.46	0.69		
	E_P	4.72	3.84	0.81	0.33	0.15	13.79	1		
MQ	***Rg***	16.41	4.98	0.30	0.07	7.21	26.9	0.92		
	Ta	8.33	11.32	1.36	-0.19	-15.46	25.72	0.93		
	Hs	8.37	1.12	0.13	0.30	5.47	11.38	0.72		
	RH	44.82	9.06	0.2	0.12	24.3	74.58	-0.29		
	Ws	2.68	0.55	0.20	0.08	1.23	4.32	0.55		
	E_P	7.26	4.45	0.61	0.10	0.42	15.89	1		
BJ	***Rg***	14.61	4.94	0.34	0.05	5.14	25.59	0.91		
	Ta	12.20	10.74	0.88	-0.17	-7.6	29.56	0.75		
	Hs	7.41	1.42	0.19	0.06	3.79	11.21	0.76		
	RH	57.29	13.70	0.24	0.02	21.86	85.52	0.09		
	Ws	2.50	0.67	0.27	0.49	1.07	4.65	0.14		
	E_P	5.09	2.83	0.56	0.70	0.85	15.63	1		
LSA	***Rg***	20.41	4.20	0.21	0.11	10.39	30.69	0.68		
	Ta	7.82	6.37	0.81	-0.21	-5.16	18.19	0.75		
	Hs	8.19	0.96	0.12	-0.59	4.66	10.55	0.18		
	RH	44.39	15.10	0.34	0.30	15.36	76.61	0.19		
	Ws	1.90	0.46	0.24	0.30	0.92	3.41	0.34		
	E_P	6.35	2.23	0.35	0.36	2.15	13.28	1		
CQ	***Rg***	8.80	4.69	0.53	0.43	0	21.32	0.92		
	Ta	17.93	7.46	0.42	-0.10	0.64	30.90	0.85		
	Hs	2.83	2.02	0.71	0.91	0	9.19	0.94		
	RH	79.15	8.55	0.11	-4.66	6.97	90.30	-0.40		
	Ws	1.36	0.34	0.25	-0.12	0.64	2.13	0.58		
	E_P	2.86	1.94	0.68	0.87	0.54	9.32	1		
HZ	***Rg***	11.63	4.20	0.36	0.54	3.93	24.83	0.94		
	Ta	16.45	8.46	0.51	-0.06	-0.01	31.03	0.88		
	Hs	4.99	1.74	0.35	0.63	1.19	11.25	0.80		
	RH	78.04	5.63	0.07	-0.80	53.74	90.42	-0.04		
	Ws	2.24	0.43	0.19	0.05	1.01	3.58	0.13		
	E_P	3.65	1.94	0.53	0.84	0.74	11.33	1		
HK	***Rg***	13.86	4.33	0.31	-0.05	4.06	24.34	0.90		
	Ta	24.08	4.07	0.17	-0.55	13.21	29.83	0.81		

Hydrol. Earth Syst. Sci. Discuss., doi:10.5194/hess-2016-247, 2016
Manuscript under review for journal Hydrol. Earth Syst. Sci.
Published: 23 May 2016

Hydrology and Earth System Sciences
Discussions

Hs	5.83	1.96	0.34	-0.26	0.47	9.94	0.89
RH	84.14	3.61	0.04	-0.52	71.39	94.46	-0.41
Ws	2.65	0.66	0.25	0.61	1.33	4.98	0.04
E_P	5.00	1.59	0.32	0.08	1.37	9.97	1

The unit of *Rg, Ta, Pa, Ws*and E_P are MJ m^{-2}, ℃,hPa,ms^{-1} and mm, respectively; x_{mean}, S_x, C_v, C_x, x_{min} and x_{max} denote the mean, standard deviation, variation coefficient, skewness, minimum and maximum values, respectively.

Table 2.The input combinations for different artificial intelligence techniques.

Models						Input combinations
ANFIS-GP	FG	GRNN	LSSV	MARS	MLP	
ANFIS-GP1	FG1	GRNN1	LSSV1	MARS1	MLP1	***Rg***
ANFIS-GP2	FG2	GRNN2	LSSV2	MARS2	MLP2	***Ta***
ANFIS-GP3	FG3	GRNN3	LSSV3	MARS3	MLP3	***Hs***
ANFIS-GP4	FG4	GRNN4	LSSV4	MARS4	MLP4	***Rg, Ta***
ANFIS-GP5	FG5	GRNN5	LSSV5	MARS5	MLP5	***Rg, Ta, Hs***
ANFIS-GP6	FG6	GRNN6	LSSV6	MARS6	MLP6	***Rg, Ta, Hs, RH***
ANFIS-GP7	FG7	GRNN7	LSSV7	MARS7	MLP7	***Rg, Ta, Hs, RH, Ws***

Hydrol. Earth Syst. Sci. Discuss., doi:10.5194/hess-2016-247, 2016
Manuscript under review for journal Hydrol. Earth Syst. Sci.
Published: 23 May 2016

Hydrology and Earth System Sciences
Discussions

636 Table 3. Comparisons of different models for predicting *Ep* at HEB.

HEB	MAE	RMSE	R^2	MAE	RMSE	R^2
ANFIS-GP1	1.062	1.411	0.815	1.044	1.431	0.819
ANFIS-GP2	1.226	1.68	0.737	1.082	1.471	0.797
ANFIS-GP3	1.589	2.05	0.609	1.496	1.834	0.726
ANFIS-GP4	0.865	1.225	0.86	0.781	1.089	0.894
ANFIS-GP5	0.785	1.167	0.873	0.645	0.907	0.923
ANFIS-GP6	0.429	0.601	0.966	0.517	0.751	0.956
ANFIS-GP7	0.378	0.521	0.975	0.431	0.6	0.967
FG1	1.031	1.371	0.825	1.031	1.507	0.816
FG2	1.151	1.632	0.752	1.077	1.502	0.786
FG3	1.528	2.008	0.625	1.354	1.798	0.74
FG4	0.719	1.071	0.893	0.688	1.178	0.891
FG5	0.67	1.002	0.907	0.673	1.059	0.897
FG6	0.39	0.56	0.971	0.474	0.69	0.961
FG7	0.305	0.421	0.983	0.435	0.661	0.959
GRNN1	1.057	1.428	0.819	1.039	1.403	0.817
GRNN2	1.155	1.632	0.753	1.057	1.475	0.796
GRNN3	1.519	2	0.628	1.379	1.816	0.738
GRNN4	0.729	1.089	0.892	0.733	1.116	0.886
GRNN5	0.703	1.042	0.901	0.652	0.988	0.908
GRNN6	0.405	0.579	0.97	0.492	0.785	0.943
GRNN7	0.343	0.483	0.979	0.499	0.745	0.951
LSSV1	1.035	1.375	0.824	1.025	1.426	0.82
LSSV2	1.131	1.619	0.756	1.062	1.491	0.79
LSSV3	1.685	2.135	0.604	1.557	1.951	0.712
LSSV4	0.675	1.007	0.906	0.703	1.099	0.89
LSSV5	0.901	1.267	0.853	0.761	1.031	0.9
LSSV6	0.556	0.812	0.941	0.591	0.864	0.934
LSSV7	0.808	1.092	0.901	0.84	1.082	0.903
MARS1	1.038	1.371	0.825	1.064	1.581	0.805
MARS2	1.067	1.523	0.784	1.098	1.584	0.767
MARS3	1.537	2.01	0.624	1.369	1.795	0.744
MARS4	0.659	0.972	0.912	0.806	1.39	0.861
MARS5	0.659	0.972	0.912	0.806	1.39	0.861
MARS6	0.548	0.72	0.952	0.596	0.959	0.931
MARS7	0.507	0.641	0.962	0.581	0.763	0.949
MLP1	1.044	1.374	0.824	1.03	1.483	0.818
MLP2	1.082	1.567	0.771	1.03	1.49	0.792
MLP3	1.135	1.618	0.757	1.04	1.46	0.798
MLP4	0.655	0.963	0.914	0.716	1.148	0.892
MLP5	0.608	0.908	0.923	0.584	0.879	0.928
MLP6	0.314	0.458	0.98	0.409	0.607	0.97
MLP7	0.279	0.398	0.985	0.314	0.405	0.988
SS	0.954	1.327	0.838	0.822	1.152	0.886
MLR	0.825	1.05	0.897	0.874	1.16	0.875

637

Hydrol. Earth Syst. Sci. Discuss., doi:10.5194/hess-2016-247, 2016
Manuscript under review for journal Hydrol. Earth Syst. Sci.
Published: 23 May 2016

Hydrology and Earth System Sciences
Discussions

638 Table 4. Comparisons of different models for predicting *Ep* at ALT.

ALT	MAE	RMSE	R^2	MAE	RMSE	R^2
ANFIS-GP1	1.19	1.597	0.841	1.003	1.268	0.896
ANFIS-GP2	1.19	1.506	0.859	1.11	1.435	0.884
ANFIS-GP3	1.345	1.763	0.807	1.214	1.601	0.844
ANFIS-GP4	0.535	0.786	0.962	0.707	1.013	0.973
ANFIS-GP5	0.494	0.737	0.966	0.691	1.012	0.977
ANFIS-GP6	0.286	0.411	0.99	0.398	0.586	0.984
ANFIS-GP7	0.241	0.351	0.992	0.371	0.545	0.987
FG1	1.079	1.398	0.878	0.994	1.3	0.891
FG2	0.78	1.065	0.929	0.953	1.29	0.928
FG3	1.052	1.375	0.882	1.002	1.328	0.92
FG4	0.45	0.703	0.969	0.67	1.027	0.971
FG5	0.49	0.717	0.968	0.697	1.043	0.971
FG6	0.266	0.38	0.991	0.391	0.575	0.987
FG7	0.253	0.343	0.993	0.394	0.57	0.988
GRNN1	1.172	1.516	0.865	0.881	1.113	0.906
GRNN2	0.875	1.223	0.913	0.882	1.187	0.927
GRNN3	1.173	1.552	0.868	0.885	1.213	0.91
GRNN4	0.532	0.84	0.957	0.663	0.936	0.977
GRNN5	0.527	0.809	0.96	0.69	0.952	0.982
GRNN6	0.192	0.301	0.994	0.47	0.657	0.989
GRNN7	0.158	0.251	0.996	0.476	0.679	0.986
LSSV1	1.077	1.421	0.875	0.928	1.212	0.9
LSSV2	0.776	1.058	0.93	0.957	1.294	0.927
LSSV3	1.063	1.381	0.881	0.986	1.299	0.92
LSSV4	0.514	0.763	0.964	0.669	0.957	0.973
LSSV5	0.481	0.732	0.967	0.669	0.974	0.978
LSSV6	0.303	0.435	0.989	0.369	0.528	0.987
LSSV7	0.39	0.587	0.98	0.487	0.647	0.986
MARS1	1.032	1.371	0.883	0.956	1.269	0.899
MARS2	0.748	1.029	0.934	0.927	1.28	0.929
MARS3	1.043	1.356	0.886	1.043	1.367	0.916
MARS4	0.437	0.657	0.973	0.641	0.996	0.975
MARS5	0.438	0.658	0.973	0.644	1.0	0.975
MARS6	0.29	0.411	0.989	0.428	0.655	0.985
MARS7	0.276	0.382	0.991	0.403	0.622	0.987
MLP1	1.03	1.363	0.884	0.951	1.268	0.897
MLP2	0.787	1.07	0.929	0.951	1.282	0.93
MLP3	0.752	1.039	0.933	0.93	1.28	0.929
MLP4	0.445	0.689	0.97	0.667	1.033	0.971
MLP5	0.521	0.769	0.963	0.659	1.017	0.974
MLP6	0.234	0.34	0.993	0.348	0.523	0.989
MLP7	0.161	0.211	0.989	0.19	0.265	0.989
SS	0.539	0.761	0.964	0.681	1.053	0.963
MLR	0.712	0.89	0.951	0.74	0.861	0.969

639

Hydrol. Earth Syst. Sci. Discuss., doi:10.5194/hess-2016-247, 2016
Manuscript under review for journal Hydrol. Earth Syst. Sci.
Published: 23 May 2016

Hydrology and Earth System Sciences
Discussions

640 Table 5. Comparisons of different models for predicting *Ep* at MQ.

MQ	MAE	RMSE	R^2	MAE	RMSE	R^2
ANFIS-GP1	1.337	1.76	0.85	1.133	1.396	0.941
ANFIS-GP2	1.33	1.698	0.86	1.203	1.587	0.863
ANFIS-GP3	2.467	3.11	0.53	2.453	3.045	0.55
ANFIS-GP4	0.83	1.178	0.933	0.868	1.22	0.952
ANFIS-GP5	0.828	1.165	0.828	0.882	1.229	0.951
ANFIS-GP6	0.648	0.886	0.962	0.608	0.81	0.981
ANFIS-GP7	0.474	0.66	0.979	0.512	0.646	0.987
FG1	1.297	1.735	0.854	1.112	1.412	0.926
FG2	1.263	1.638	0.87	1.198	1.555	0.87
FG3	2.447	3.057	0.546	2.373	2.953	0.58
FG4	0.828	1.178	0.933	0.854	1.196	0.952
FG5	0.795	1.13	0.938	0.923	1.335	0.942
FG6	0.608	0.81	0.968	0.636	0.805	0.978
FG7	0.456	0.614	0.983	0.435	0.574	0.99
GRNN1	1.427	1.814	0.854	1.071	1.315	0.925
GRNN2	1.225	1.593	0.877	1.148	1.504	0.876
GRNN3	2.663	3.15	0.542	2.381	2.821	0.596
GRNN4	0.733	1.056	0.946	0.78	1.089	0.954
GRNN5	0.647	0.944	0.957	0.815	1.161	0.951
GRNN6	0.329	0.486	0.989	0.634	0.892	0.972
GRNN7	0.248	0.392	0.993	0.548	0.74	0.981
LSSV1	1.343	1.758	0.85	1.094	1.368	0.935
LSSV2	1.274	1.643	0.869	1.187	1.548	0.869
LSSV3	2.46	3.057	0.547	2.383	2.942	0.574
LSSV4	1.06	1.365	0.925	0.93	1.107	0.951
LSSV5	0.815	1.143	0.937	0.9	1.225	0.945
LSSV6	0.934	1.193	0.94	0.891	1.089	0.962
LSSV7	0.888	1.113	0.95	0.767	0.927	0.97
MARS1	1.291	1.728	0.855	1.092	1.404	0.928
MARS2	1.076	1.462	0.896	1.078	1.471	0.888
MARS3	2.419	3.039	0.552	2.436	2.996	0.564
MARS4	0.815	1.144	0.936	0.922	1.23	0.947
MARS5	0.807	1.126	0.938	0.97	1.29	0.95
MARS6	0.668	0.87	0.963	0.735	0.929	0.973
MARS7	0.546	0.72	0.975	0.627	0.826	0.977
MLP1	1.297	1.735	0.854	1.107	1.408	0.928
MLP2	1.057	1.458	0.897	1.113	1.492	0.888
MLP3	1.139	1.524	0.887	1.108	1.488	0.884
MLP4	0.724	1.026	0.949	0.797	1.074	0.96
MLP5	0.742	1.064	0.945	0.821	1.113	0.959
MLP6	0.538	0.738	0.974	0.538	0.716	0.981
MLP7	0.384	0.532	0.986	0.358	0.489	0.99
SS	0.922	1.281	0.92	1.039	1.389	0.944
MLR	0.77	0.967	0.955	0.784	0.921	0.972

641

Hydrol. Earth Syst. Sci. Discuss., doi:10.5194/hess-2016-247, 2016
Manuscript under review for journal Hydrol. Earth Syst. Sci.
Published: 23 May 2016

Hydrology and Earth System Sciences
Discussions

642 Table 6. Comparisons of different models for predicting *Ep* at BJ.

BJ	MAE	RMSE	R^2	MAE	RMSE	R^2
ANFIS-GP1	0.872	1.205	0.826	0.749	0.956	0.922
ANFIS-GP2	1.439	1.907	0.564	1.294	1.554	0.662
ANFIS-GP3	1.431	1.818	0.603	1.482	1.88	0.561
ANFIS-GP4	0.846	1.189	0.831	0.717	0.923	0.921
ANFIS-GP5	0.742	1.071	0.862	0.688	0.972	0.909
ANFIS-GP6	0.464	0.735	0.935	0.384	0.51	0.965
ANFIS-GP7	0.424	0.657	0.948	0.361	0.48	0.971
FG1	0.835	1.127	0.848	0.823	1.075	0.914
FG2	1.416	1.891	0.571	1.256	1.544	0.665
FG3	1.387	1.733	0.64	1.483	1.846	0.561
FG4	0.742	1.063	0.864	0.688	0.997	0.922
FG5	0.721	1.052	0.867	0.679	0.959	0.926
FG6	0.451	0.721	0.938	0.394	0.484	0.971
FG7	0.431	0.655	0.949	0.431	0.586	0.963
GRNN1	0.819	1.114	0.852	0.811	1.062	0.916
GRNN2	1.379	1.852	0.589	1.23	1.52	0.678
GRNN3	1.374	1.727	0.647	1.491	1.843	0.564
GRNN4	0.626	0.924	0.898	0.657	0.939	0.904
GRNN5	0.665	0.998	0.882	0.639	0.947	0.914
GRNN6	0.32	0.533	0.966	0.391	0.513	0.962
GRNN7	0.166	0.301	0.989	0.356	0.473	0.968
LSSV1	0.842	1.139	0.845	0.824	1.062	0.911
LSSV2	1.519	1.986	0.552	1.441	1.658	0.647
LSSV3	1.386	1.734	0.64	1.483	1.841	0.562
LSSV4	0.743	1.069	0.864	0.69	0.977	0.922
LSSV5	0.823	1.184	0.839	0.692	0.958	0.911
LSSV6	0.736	1.078	0.875	0.622	0.827	0.925
LSSV7	0.486	0.76	0.933	0.338	0.444	0.973
MARS1	0.829	1.118	0.85	0.854	1.071	0.915
MARS2	1.364	1.832	0.597	1.282	1.607	0.659
MARS3	1.355	1.717	0.647	1.477	1.846	0.565
MARS4	0.705	0.979	0.885	0.68	0.976	0.909
MARS5	0.687	0.972	0.887	0.687	0.991	0.903
MARS6	0.52	0.767	0.929	0.5	0.603	0.963
MARS7	0.478	0.717	0.938	0.427	0.527	0.971
MLP1	0.784	1.075	0.861	0.813	1.045	0.914
MLP2	1.325	1.803	0.61	1.249	1.595	0.677
MLP3	1.401	1.875	0.578	1.236	1.523	0.678
MLP4	0.675	0.968	0.888	0.66	0.974	0.911
MLP5	0.653	0.962	0.889	0.62	0.907	0.904
MLP6	0.417	0.692	0.943	0.312	0.394	0.982
MLP7	0.337	0.506	0.969	0.314	0.428	0.979
SS	0.89	1.263	0.816	0.647	0.921	0.897
MLR	0.614	0.879	0.907	0.514	0.648	0.946

643

Hydrol. Earth Syst. Sci. Discuss., doi:10.5194/hess-2016-247, 2016
Manuscript under review for journal Hydrol. Earth Syst. Sci.
Published: 23 May 2016

644 Table 7. Comparisons of different models for predicting *Ep* at LSA.

LSA	MAE	RMSE	R^2	MAE	RMSE	R^2
ANFIS-GP1	1.327	1.718	0.411	1.072	1.424	0.594
ANFIS-GP2	1.245	1.523	0.536	1.192	1.417	0.601
ANFIS-GP3	1.821	2.218	0.017	1.796	2.148	0.055
ANFIS-GP4	1.149	1.471	0.568	1.046	1.304	0.651
ANFIS-GP5	0.966	1.223	0.701	0.875	1.082	0.761
ANFIS-GP6	0.529	0.675	0.909	0.73	0.907	0.896
ANFIS-GP7	0.478	0.61	0.926	0.816	1.038	0.875
FG1	1.324	1.715	0.413	1.073	1.415	0.6
FG2	1.151	1.465	0.571	1.159	1.392	0.621
FG3	1.803	2.169	0.06	1.771	2.093	0.118
FG4	1.044	1.381	0.619	0.987	1.201	0.725
FG5	0.968	1.215	0.705	0.896	1.099	0.757
FG6	0.499	0.631	0.921	0.767	0.925	0.903
FG7	0.491	0.61	0.926	0.729	0.886	0.914
GRNN1	1.296	1.692	0.429	1.094	1.436	0.587
GRNN2	1.025	1.336	0.647	1.072	1.288	0.679
GRNN3	1.783	2.152	0.077	1.762	2.08	0.134
GRNN4	0.841	1.131	0.751	0.817	1.032	0.795
GRNN5	0.639	0.844	0.862	0.714	0.937	0.828
GRNN6	0.33	0.427	0.965	0.533	0.65	0.926
GRNN7	0.326	0.417	0.967	0.459	0.592	0.933
LSSV1	1.376	1.754	0.41	1.211	1.508	0.599
LSSV2	1.22	1.499	0.554	1.213	1.422	0.606
LSSV3	1.811	2.209	0.027	1.791	2.144	0.07
LSSV4	1.163	1.476	0.573	1.078	1.31	0.663
LSSV5	0.987	1.253	0.69	0.894	1.085	0.777
LSSV6	0.462	0.601	0.933	0.646	0.799	0.916
LSSV7	0.47	0.609	0.932	0.591	0.713	0.928
MARS1	1.316	1.713	0.414	1.072	1.412	0.602
MARS2	1.012	1.318	0.653	1.098	1.299	0.683
MARS3	1.82	2.182	0.049	1.766	2.089	0.12
MARS4	0.917	1.23	0.698	0.947	1.176	0.735
MARS5	0.94	1.227	0.699	0.913	1.135	0.746
MARS6	0.501	0.641	0.918	0.762	0.929	0.91
MARS7	0.528	0.66	0.913	0.697	0.85	0.92
MLP1	1.308	1.707	0.418	1.073	1.413	0.596
MLP2	0.992	1.307	0.659	1.111	1.313	0.675
MLP3	0.994	1.316	0.654	1.108	1.312	0.675
MLP4	0.883	1.187	0.719	0.918	1.123	0.754
MLP5	0.686	0.91	0.835	0.728	0.958	0.825
MLP6	0.397	0.503	0.949	0.629	0.771	0.928
MLP7	0.522	0.681	0.907	0.53	0.638	0.936
SS	1.198	1.577	0.515	0.969	1.307	0.652
MLR	0.628	0.795	0.874	0.656	0.789	0.906

645

Hydrol. Earth Syst. Sci. Discuss., doi:10.5194/hess-2016-247, 2016
Manuscript under review for journal Hydrol. Earth Syst. Sci.
Published: 23 May 2016

646 Table 8. Comparisons of different models for predicting *Ep* at CQ.

CQ	MAE	RMSE	R^2	MAE	RMSE	R^2
ANFIS-GP1	0.466	0.859	0.815	0.28	0.397	0.958
ANFIS-GP2	0.82	1.189	0.645	0.693	0.959	0.748
ANFIS-GP3	0.539	0.722	0.869	0.537	0.679	0.876
ANFIS-GP4	0.416	0.786	0.845	0.316	0.398	0.959
ANFIS-GP5	0.369	0.492	0.939	0.242	0.329	0.968
ANFIS-GP6	0.225	0.29	0.979	0.224	0.312	0.976
ANFIS-GP7	0.187	0.244	0.985	0.203	0.3	0.978
FG1	0.467	0.805	0.837	0.294	0.375	0.963
FG2	0.611	0.881	0.805	0.571	0.691	0.873
FG3	0.474	0.672	0.887	0.479	0.607	0.905
FG4	0.385	0.704	0.876	0.303	0.384	0.96
FG5	0.297	0.402	0.959	0.273	0.19	0.944
FG6	0.275	0.359	0.968	0.3	0.407	0.955
FG7	0.195	0.25	0.984	0.182	0.28	0.981
GRNN1	0.437	0.746	0.861	0.284	0.374	0.963
GRNN2	0.574	0.845	0.823	0.507	0.651	0.883
GRNN3	0.453	0.652	0.893	0.473	0.61	0.902
GRNN4	0.328	0.645	0.897	0.285	0.37	0.962
GRNN5	0.221	0.308	0.976	0.24	0.327	0.968
GRNN6	0.145	0.203	0.99	0.177	0.24	0.983
GRNN7	0.227	0.308	0.977	0.234	0.297	0.975
LSSV1	0.714	1.028	0.81	0.6	0.734	0.961
LSSV2	0.552	0.825	0.829	0.503	0.65	0.888
LSSV3	0.687	0.862	0.887	0.625	0.765	0.906
LSSV4	0.543	0.873	0.833	0.449	0.58	0.94
LSSV5	0.336	0.48	0.942	0.292	0.372	0.959
LSSV6	0.314	0.496	0.94	0.219	0.284	0.977
LSSV7	0.317	0.49	0.942	0.22	0.292	0.976
MARS1	0.451	0.709	0.874	0.28	0.441	0.943
MARS2	0.555	0.822	0.83	0.498	0.651	0.889
MARS3	0.453	0.664	0.889	0.466	0.599	0.904
MARS4	0.363	0.624	0.902	0.33	0.441	0.95
MARS5	0.336	0.48	0.942	0.292	0.372	0.959
MARS6	0.273	0.426	0.954	0.219	0.299	0.974
MARS7	0.267	0.417	0.956	0.25	0.323	0.956
MLP1	0.419	0.733	0.865	0.27	0.371	0.96
MLP2	0.55	0.81	0.835	0.509	0.658	0.887
MLP3	0.568	0.845	0.82	0.502	0.637	0.893
MLP4	0.334	0.65	0.894	0.266	0.355	0.966
MLP5	0.252	0.348	0.97	0.218	0.296	0.975
MLP6	0.185	0.239	0.986	0.167	0.23	0.985
MLP7	0.161	0.211	0.989	0.189	0.265	0.985
SS	0.379	0.786	0.847	0.226	0.307	0.973
MLR	0.389	0.534	0.928	0.317	0.398	0.955

647

Hydrol. Earth Syst. Sci. Discuss., doi:10.5194/hess-2016-247, 2016
Manuscript under review for journal Hydrol. Earth Syst. Sci.
Published: 23 May 2016

Hydrology and Earth System Sciences
Discussions

Table 9. Comparisons of different models for predicting *Ep* at HZ station.

	MAE	RMSE	R^2	MAE	RMSE	R^2
ANFIS-GP1	0.532	0.698	0.87	0.451	0.605	0.903
ANFIS-GP2	0.72	1.001	0.734	0.728	0.965	0.754
ANFIS-GP3	0.937	1.164	0.64	0.991	1.178	0.694
ANFIS-GP4	0.377	0.521	0.928	0.333	0.448	0.948
ANFIS-GP5	0.357	0.482	0.938	0.311	0.397	0.961
ANFIS-GP6	0.272	0.356	0.966	0.329	0.427	0.965
ANFIS-GP7	0.242	0.312	0.974	0.347	0.453	0.949
FG1	0.519	0.686	0.875	0.438	0.59	0.908
FG2	0.62	0.817	0.822	0.626	0.786	0.837
FG3	0.943	1.151	0.648	1.01	1.188	0.699
FG4	0.358	0.485	0.938	0.299	0.397	0.959
FG5	0.344	0.462	0.943	0.29	0.373	0.965
FG6	0.269	0.347	0.968	0.295	0.375	0.974
FG7	0.26	0.36	0.966	0.278	0.369	0.964
GRNN1	0.519	0.68	0.878	0.457	0.607	0.904
GRNN2	0.556	0.733	0.859	0.581	0.736	0.86
GRNN3	0.926	1.127	0.664	1.02	1.197	0.705
GRNN4	0.322	0.438	0.949	0.314	0.409	0.957
GRNN5	0.238	0.327	0.972	0.295	0.404	0.961
GRNN6	0.232	0.3	0.977	0.275	0.346	0.969
GRNN7	0.223	0.295	0.978	0.335	0.445	0.956
LSSV1	0.593	0.801	0.87	0.572	0.731	0.903
LSSV2	0.715	0.984	0.778	0.733	0.97	0.799
LSSV3	0.996	1.214	0.638	1.074	1.267	0.678
LSSV4	0.413	0.594	0.924	0.399	0.548	0.94
LSSV5	0.398	0.554	0.929	0.376	0.509	0.953
LSSV6	0.278	0.378	0.964	0.3	0.372	0.968
LSSV7	0.292	0.406	0.959	0.338	0.441	0.957
MARS1	0.52	0.69	0.874	0.443	0.601	0.904
MARS2	0.534	0.686	0.875	0.524	0.673	0.881
MARS3	0.915	1.125	0.664	0.999	1.189	0.698
MARS4	0.339	0.449	0.946	0.273	0.362	0.966
MARS5	0.335	0.437	0.949	0.282	0.358	0.966
MARS6	0.286	0.37	0.964	0.318	0.393	0.976
MARS7	0.27	0.358	0.966	0.276	0.361	0.967
MLP1	0.529	0.691	0.873	0.449	0.598	0.906
MLP2	0.523	0.68	0.877	0.523	0.674	0.881
MLP3	0.908	1.124	0.664	0.992	1.181	0.698
MLP4	0.334	0.65	0.894	0.266	0.355	0.966
MLP5	0.333	0.446	0.947	0.279	0.348	0.968
MLP6	0.247	0.326	0.972	0.318	0.405	0.978
MLP7	0.244	0.319	0.973	0.263	0.34	0.977
SS	0.35	0.487	0.938	0.291	0.388	0.96
MLR	0.32	0.427	0.952	0.395	0.486	0.942

Hydrol. Earth Syst. Sci. Discuss., doi:10.5194/hess-2016-247, 2016
Manuscript under review for journal Hydrol. Earth Syst. Sci.
Published: 23 May 2016

650 Table 10. Comparisons of different models for predicting *Ep* at HK.

HK	MAE	RMSE	R^2	MAE	RMSE	R^2
ANFIS-GP1	0.528	0.688	0.814	0.669	0.8	0.854
ANFIS-GP2	0.741	0.964	0.634	0.802	0.97	0.742
ANFIS-GP3	0.619	0.798	0.749	0.482	0.61	0.851
ANFIS-GP4	0.488	0.646	0.836	0.66	0.796	0.861
ANFIS-GP5	0.46	0.597	0.86	0.494	0.609	0.891
ANFIS-GP6	0.388	0.501	0.901	0.809	0.93	0.919
ANFIS-GP7	0.286	0.379	0.943	0.428	0.555	0.925
FG1	0.506	0.661	0.828	0.662	0.792	0.858
FG2	0.716	0.914	0.671	0.793	0.94	0.784
FG3	0.612	0.768	0.768	0.503	0.63	0.85
FG4	0.471	0.626	0.846	0.659	0.786	0.875
FG5	0.451	0.591	0.863	0.485	0.596	0.895
FG6	0.39	0.496	0.903	0.718	0.849	0.92
FG7	0.381	0.494	0.904	0.452	0.566	0.886
GRNN1	0.505	0.666	0.829	0.673	0.81	0.854
GRNN2	0.699	0.902	0.681	0.786	0.929	0.776
GRNN3	0.6	0.759	0.775	0.511	0.642	0.845
GRNN4	0.452	0.605	0.859	0.65	0.771	0.879
GRNN5	0.405	0.535	0.889	0.484	0.589	0.892
GRNN6	0.408	0.538	0.894	0.539	0.651	0.916
GRNN7	0.241	0.342	0.956	0.415	0.512	0.917
LSSV1	0.51	0.671	0.826	0.659	0.791	0.859
LSSV2	0.717	0.924	0.665	0.788	0.934	0.78
LSSV3	0.614	0.781	0.766	0.519	0.643	0.852
LSSV4	0.481	0.64	0.841	0.661	0.789	0.87
LSSV5	0.446	0.583	0.867	0.483	0.596	0.891
LSSV6	0.414	0.528	0.891	0.625	0.748	0.919
LSSV7	0.313	0.41	0.935	0.419	0.529	0.918
MARS1	0.505	0.662	0.828	0.665	0.79	0.862
MARS2	0.664	0.862	0.708	0.858	1.023	0.766
MARS3	0.603	0.758	0.774	0.5	0.632	0.845
MARS4	0.438	0.581	0.867	0.733	0.899	0.869
MARS5	0.426	0.547	0.882	0.536	0.691	0.891
MARS6	0.407	0.517	0.895	0.682	0.807	0.917
MARS7	0.322	0.414	0.932	0.397	0.515	0.927
MLP1	0.512	0.671	0.823	0.657	0.793	0.855
MLP2	0.686	0.878	0.697	0.822	0.979	0.792
MLP3	0.707	0.903	0.679	0.821	0.973	0.79
MLP4	0.47	0.623	0.847	0.657	0.779	0.878
MLP5	0.421	0.542	0.884	0.485	0.594	0.897
MLP6	0.431	0.554	0.88	0.671	0.786	0.916
MLP7	0.34	0.444	0.923	0.386	0.491	0.930
SS	0.523	0.683	0.827	0.64	0.773	0.823
MLR	0.328	0.431	0.927	0.396	0.505	0.927

651
652

Hydrol. Earth Syst. Sci. Discuss., doi:10.5194/hess-2016-247, 2016
Manuscript under review for journal Hydrol. Earth Syst. Sci.
Published: 23 May 2016

Hydrology and Earth System Sciences
Discussions
Open Access
EGU

Table 11. Accuracy ranks of the soft computing models in estimating *Ep*.

Stations	ANFIS-GP	FG	GRNN	LSSVR	MARS	MLP	MLR
HEB	2	3	4	6	5	1	7
ALT	3	4	6	2	5	1	7
MQ	3	2	4	7	5	1	6
BJ	4	5	3	2	6	1	7
LSA	6	5	1	3	4	2	7
CQ	6	3	2	4	5	1	7
HZ	6	4	2	5	3	1	7
HK	6	7	3	5	4	1	2
ALL	4	5	2	3	6	1	7
Total	**40**	**38**	**27**	**37**	**43**	**10**	**57**

Hydrol. Earth Syst. Sci. Discuss., doi:10.5194/hess-2016-247, 2016
Manuscript under review for journal Hydrol. Earth Syst. Sci.
Published: 23 May 2016

695 Table 12. Comparisons of different models for predicting *Ep* at all stations.

	MAE	RMSE	R^2	MAE	RMSE	R^2
ANFIS-GP1	1.204	1.681	0.739	1.022	1.378	0.804
ANFIS-GP2	1.906	2.522	0.412	1.768	2.345	0.437
ANFIS-GP3	1.913	2.377	0.478	1.877	2.262	0.475
ANFIS-GP4	0.994	1.446	0.807	0.88	1.228	0.847
ANFIS-GP5	0.917	1.341	0.834	0.782	1.113	0.872
ANFIS-GP6	0.606	0.846	0.934	0.601	0.833	0.933
ANFIS-GP7	0.517	0.738	0.95	0.486	0.666	0.957
FG1	1.208	1.676	0.74	1.028	1.377	0.805
FG2	1.883	2.511	0.417	1.741	2.332	0.443
FG3	1.8	2.221	0.544	1.812	2.148	0.524
FG4	0.936	1.378	0.824	0.821	1.154	0.865
FG5	0.883	1.294	0.845	0.753	1.072	0.882
FG6	0.589	0.834	0.936	0.607	0.842	0.931
FG7	0.518	0.744	0.949	0.495	0.678	0.956
GRNN1	1.193	1.669	0.743	1.013	1.373	0.806
GRNN2	1.859	2.49	0.427	1.716	2.311	0.453
GRNN3	1.772	2.216	0.549	1.773	2.127	0.532
GRNN4	0.819	1.234	0.86	0.733	1.075	0.884
GRNN5	0.724	1.114	0.886	0.642	0.963	0.905
GRNN6	0.458	0.674	0.958	0.489	0.723	0.947
GRNN7	0.265	0.425	0.984	0.364	0.573	0.967
LSSV1	1.198	1.667	0.743	1.017	1.371	0.807
LSSV2	1.85	2.495	0.425	1.703	2.312	0.453
LSSV3	1.854	2.314	0.506	1.858	2.215	0.493
LSSV4	0.935	1.386	0.823	0.806	1.149	0.866
LSSV5	0.933	1.369	0.827	0.8	1.134	0.867
LSSV6	0.824	1.148	0.879	0.774	1.023	0.893
LSSV7	0.494	0.719	0.952	0.476	0.657	0.958
MARS1	1.198	1.666	0.744	1.021	1.373	0.806
MARS2	1.793	2.428	0.455	1.676	2.268	0.476
MARS3	1.782	2.209	0.549	1.788	2.131	0.532
MARS4	1.025	1.439	0.808	0.929	1.235	0.845
MARS5	0.925	1.324	0.838	0.804	1.113	0.873
MARS6	0.783	1.032	0.902	0.76	0.963	0.909
MARS7	0.692	0.933	0.920	0.654	0.829	0.932
MLP1	1.196	1.663	0.744	1.02	1.373	0.806
MLP2	1.835	2.485	0.429	1.689	2.304	0.457
MLP3	1.842	2.491	0.426	1.695	2.302	0.458
MLP4	0.836	1.256	0.854	0.74	1.086	0.882
MLP5	0.774	1.181	0.871	0.649	0.98	0.902
MLP6	0.529	0.758	0.947	0.531	0.77	0.943
MLP7	0.279	0.398	0.985	0.314	0.405	0.988
SS	1.107	1.544	0.785	1.007	1.336	0.823
MLR	0.905	1.235	0.859	0.86	1.091	0.88

696
697

Hydrol. Earth Syst. Sci. Discuss., doi:10.5194/hess-2016-247, 2016
Manuscript under review for journal Hydrol. Earth Syst. Sci.
Published: 23 May 2016

Figure captions:

Fig.1. Schematic architecture of: a) MLP neural network; b) GRNN.

Fig.2. Schematic architecture of network-based ANFIS.

Fig.3. The geographical locations of the stations in different climatic zones.

Fig.4. The annual variations of *Ep* and associated climatic parameters in each station.

Fig.5. Monthly variations of *Ep* and associated climatic parameters in each station.

Fig.6. Comparison of the observed and estimated *Ep* using the optimal ANFIS-GP model during the testing period.

Fig.7. Comparison of the observed and estimated *Ep* using the optimal FG model during the testing period.

Fig.8. Comparison of the observed and estimated *Ep* using the optimal GRNN model during the testing period.

Fig.9. Comparison of the observed and estimated *Ep* using the optimal LSSVM model during the testing period.

Fig.10. Comparison of the observed and estimated *Ep* using the optimal MARS model during the testing period.

Fig.11. Comparison of the observed and estimated *Ep* using the optimal MLP model during the testing period.

Fig.12. Comparison of the observed and estimated *Ep* using the optimal SS model during the testing period.

Fig.13. Comparison of the observed and estimated *Ep* using the optimal MLR model during the testing period.

Hydrol. Earth Syst. Sci. Discuss., doi:10.5194/hess-2016-247, 2016
Manuscript under review for journal Hydrol. Earth Syst. Sci.
Published: 23 May 2016

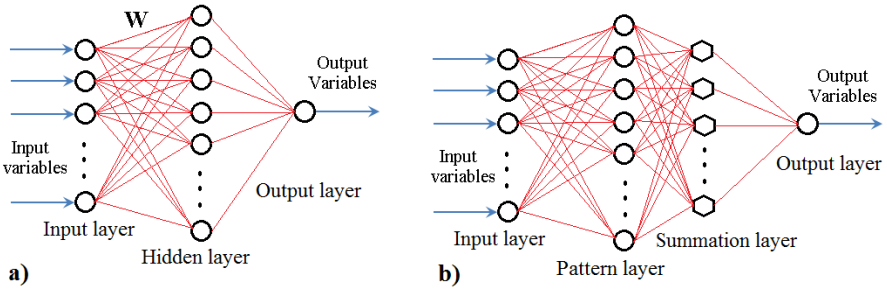

Fig. 1. Schematic architecture of: a) MLP neural network; b) GRNN.

Hydrol. Earth Syst. Sci. Discuss., doi:10.5194/hess-2016-247, 2016
Manuscript under review for journal Hydrol. Earth Syst. Sci.
Published: 23 May 2016

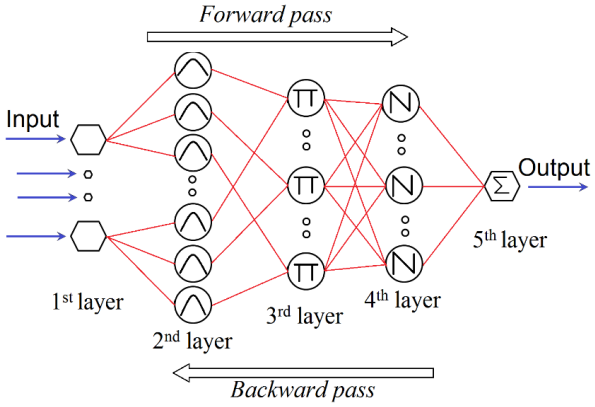

Fig. 2. Schematic architecture of network-based ANFIS.

Hydrol. Earth Syst. Sci. Discuss., doi:10.5194/hess-2016-247, 2016
Manuscript under review for journal Hydrol. Earth Syst. Sci.
Published: 23 May 2016

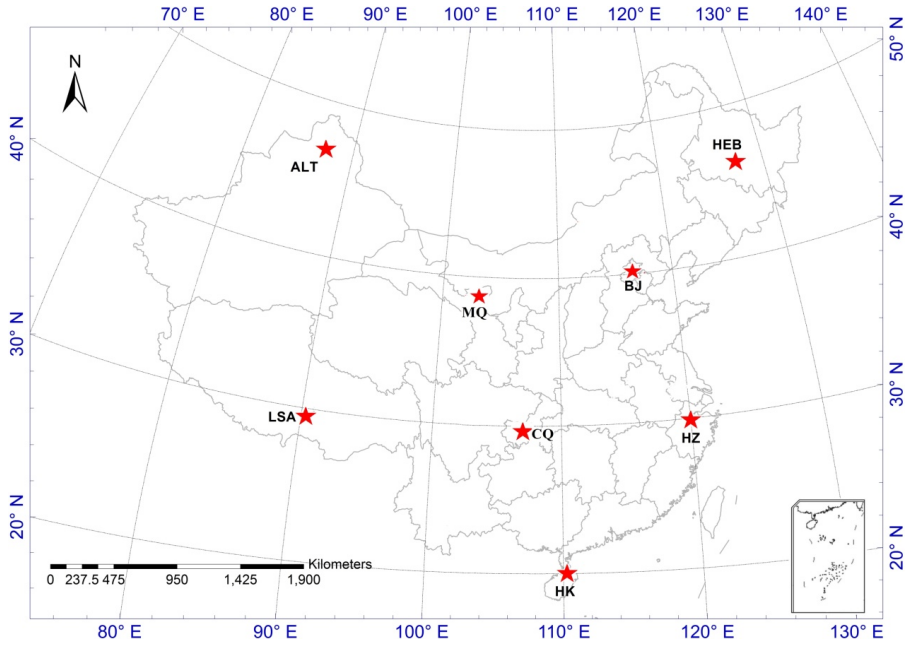

Fig.3. The geographical locations of the stations in different climatic zones.

Hydrol. Earth Syst. Sci. Discuss., doi:10.5194/hess-2016-247, 2016
Manuscript under review for journal Hydrol. Earth Syst. Sci.
Published: 23 May 2016

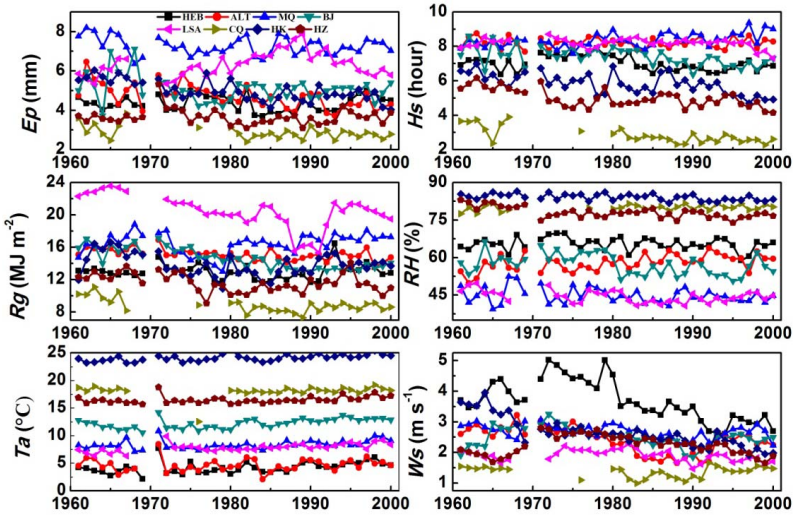

Fig.4. The annual variations of *Ep* and associated climatic parameters in each station.

Hydrol. Earth Syst. Sci. Discuss., doi:10.5194/hess-2016-247, 2016
Manuscript under review for journal Hydrol. Earth Syst. Sci.
Published: 23 May 2016

875

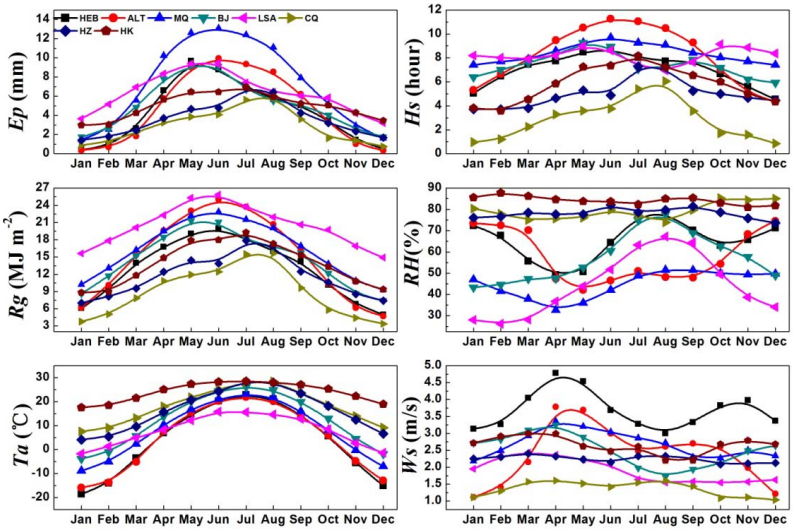

876

877 Fig.5. Monthly variations of *Ep* and associated climatic parameters in each station.

878
879
880
881
882
883
884
885
886
887
888
889
890
891
892
893
894
895
896
897

Hydrol. Earth Syst. Sci. Discuss., doi:10.5194/hess-2016-247, 2016
Manuscript under review for journal Hydrol. Earth Syst. Sci.
Published: 23 May 2016

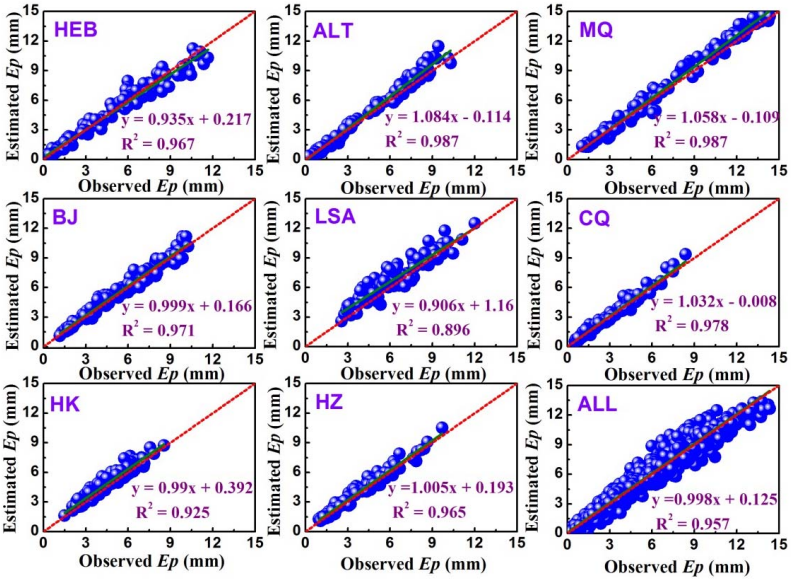

Fig.6. Comparison of the observed and estimated *Ep* using the optimal ANFIS-GP model during the testing period.

Hydrol. Earth Syst. Sci. Discuss., doi:10.5194/hess-2016-247, 2016
Manuscript under review for journal Hydrol. Earth Syst. Sci.
Published: 23 May 2016

923

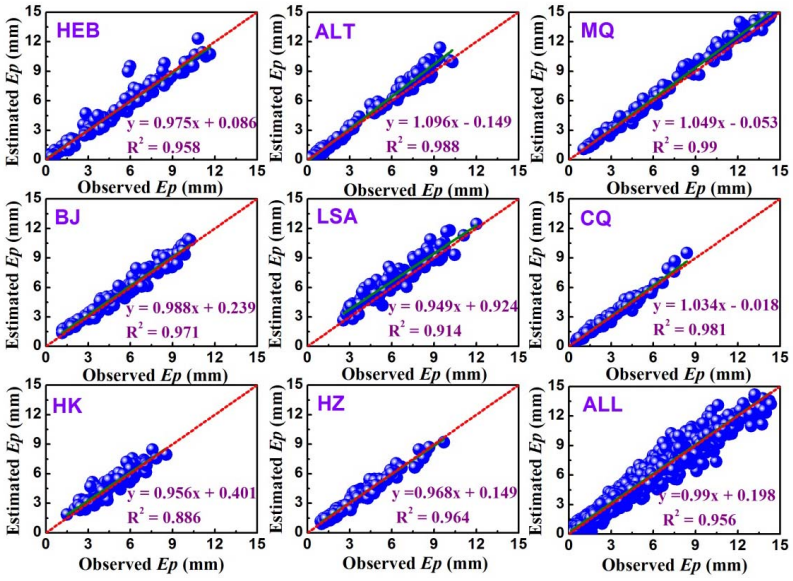

924

925 Fig.7. Comparison of the observed and estimated *Ep* using the optimal FG model during the
926 testing period.

927
928
929
930
931
932
933
934
935
936
937
938
939
940
941
942
943
944
945

Hydrol. Earth Syst. Sci. Discuss., doi:10.5194/hess-2016-247, 2016
Manuscript under review for journal Hydrol. Earth Syst. Sci.
Published: 23 May 2016

946

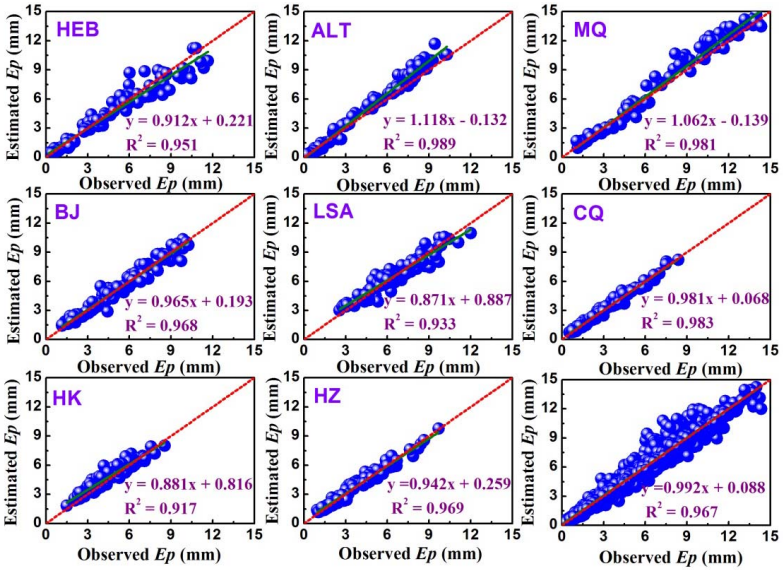

947

948 Fig.8. Comparison of the observed and estimated *Ep* using the optimal GRNN model during

949 the testing period.

950
951
952
953
954
955
956
957
958
959
960
961
962
963
964
965
966
967
968
969
970

Hydrol. Earth Syst. Sci. Discuss., doi:10.5194/hess-2016-247, 2016
Manuscript under review for journal Hydrol. Earth Syst. Sci.
Published: 23 May 2016

971

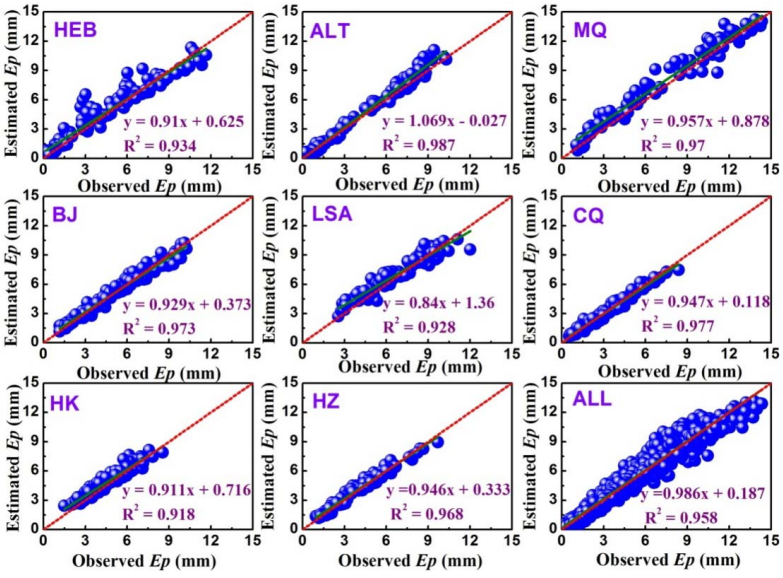

972

973 Fig.9. Comparison of the observed and estimated *Ep* using the optimal LSSVM model during
974 the testing period.

975
976
977
978
979
980
981
982
983
984
985
986
987
988
989
990
991
992
993
994
995
996
997

Hydrol. Earth Syst. Sci. Discuss., doi:10.5194/hess-2016-247, 2016
Manuscript under review for journal Hydrol. Earth Syst. Sci.
Published: 23 May 2016

998

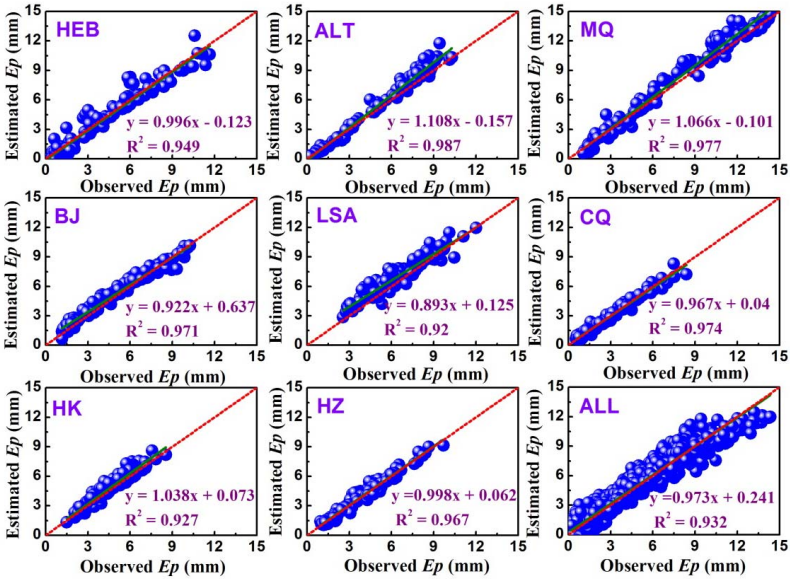

999

1000 Fig.10. Comparison of the observed and estimated *Ep* using the optimal MARS model during
1001 the testing period.

1002
1003
1004
1005
1006
1007
1008
1009
1010
1011
1012
1013
1014
1015
1016
1017
1018
1019
1020
1021

Hydrol. Earth Syst. Sci. Discuss., doi:10.5194/hess-2016-247, 2016
Manuscript under review for journal Hydrol. Earth Syst. Sci.
Published: 23 May 2016

1022

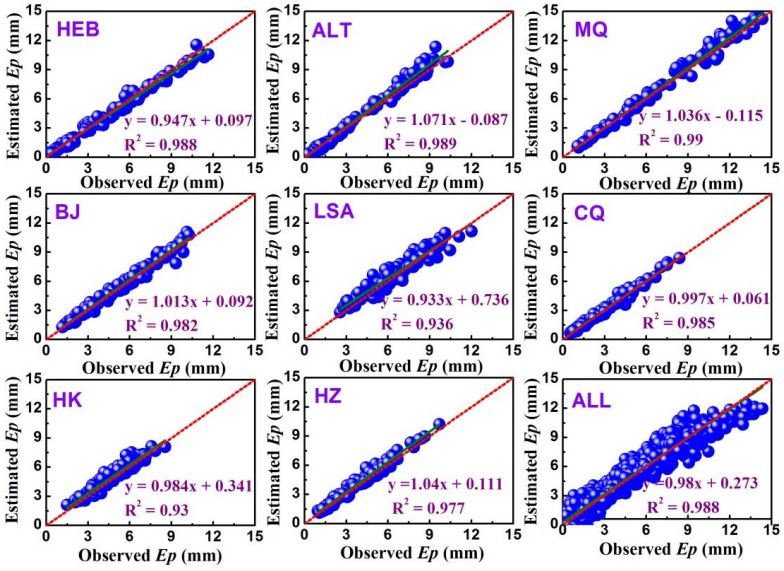

1023

1024 Fig.11. Comparison of the observed and estimated *Ep* using the optimal MLP model during

1025 the testing period.

1026
1027
1028
1029
1030
1031
1032
1033
1034
1035
1036
1037
1038
1039
1040
1041
1042
1043
1044

Hydrol. Earth Syst. Sci. Discuss., doi:10.5194/hess-2016-247, 2016
Manuscript under review for journal Hydrol. Earth Syst. Sci.
Published: 23 May 2016

1045

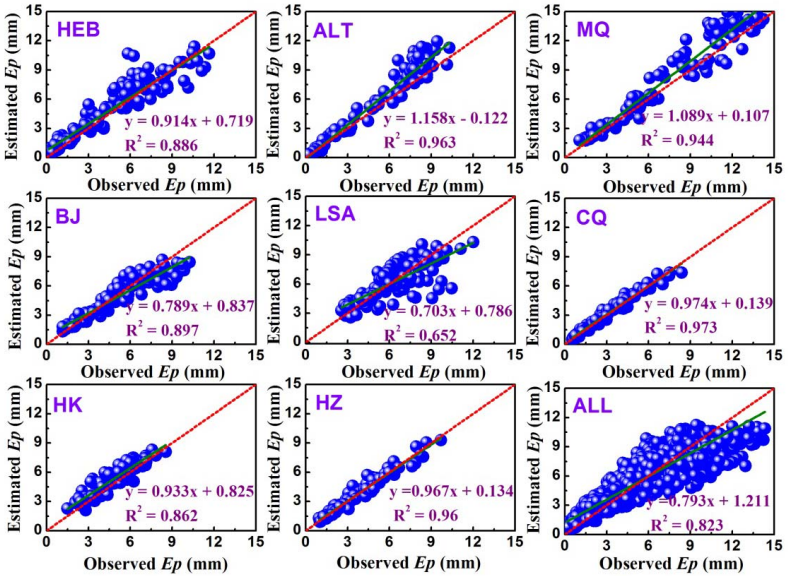

1046

1047 Fig.12. Comparison of the observed and estimated *Ep* using the optimal SS model during the

1048 testing period.

1049
1050
1051
1052
1053
1054
1055
1056
1057
1058
1059
1060
1061
1062
1063
1064
1065
1066
1067
1068
1069
1070

Hydrol. Earth Syst. Sci. Discuss., doi:10.5194/hess-2016-247, 2016
Manuscript under review for journal Hydrol. Earth Syst. Sci.
Published: 23 May 2016

1071

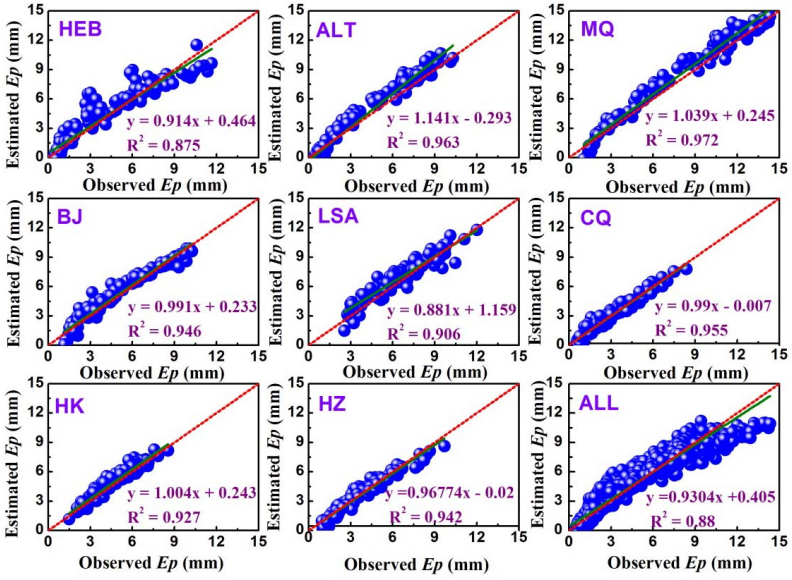

1072

1073 Fig.13. Comparison of the observed and estimated *Ep* using the optimal MLR model during
1074 the testing period.

1075

1076